State of the Climate in Asia

2020

WEATHER CLIMATE WATER

WORLD METEOROLOGICAL ORGANIZATION

WMO-No. 1273

WMO-No. 1273

Chair, Publications Board
World Meteorological Organization (WMO)
7 bis, avenue de la Paix
P.O. Box 2300
CH-1211 Geneva 2, Switzerland

Tel.: +41 (0) 22 730 84 03
Fax: +41 (0) 22 730 81 17
Email: publications@wmo.int

ISBN 978-92-63-11273-6

Contents

Foreword

The State of the Climate (SoC) in Asia 2020 is the first of its kind, multi-agency effort to provide science-based knowledge on the state of climate in Asia and its inter-connection with sustainable development in the region. The report highlights the major climate trends through universally agreed climate change indicators, addressing land and sea temperatures, glacial retreat, sea level rise, and decreasing sea-ice extent in addition to high impact events which affected the region during 2020.

Weather and climate hazards, especially floods, storms, and droughts, highlighted in the report, had significant impacts in many countries of the region—affecting agriculture and food security, contributing to increased displacement and vulnerability of migrants, refugees, and displaced people, worsening health risks, and exacerbating environmental issues and losses of natural ecosystems. Combined, these impacts take a significant toll on long term sustainable development, and progress toward the UN 2030 Agenda and Sustainable Development Goals in particular.

The information contained in this report is intended to help to better understand the climate trends and events, extreme weather, and the associated risks and impacts in the region. Climate change often acts as a threat multiplier to poverty, through cascading effects and compounding risks that need to be addressed in disaster risk reduction efforts. Enhanced monitoring of climate drivers at regional scales and increased funding for climate observing and early warning systems, and associated services are crucial elements for developing climate resilient economies and societies which have become more necessary than ever to "build back better" from the COVID-19 pandemic.

I congratulate the lead authors of their scientific coordination of this report, as well as the individuals and institutions who contributed, and would especially like to thank sister United Nations agencies for their collaboration.

Prof. Petteri Taalas
Secretary General

Key messages

The Asia mean temperature for 2020 was 1.39 °C above the 1981–2010 average, which places 2020 as the warmest year on record in all data sets used for this assessment. The spread of the estimates ranges between 1.29 °C and 1.55 °C. The land surface temperature, sea-surface temperature and ocean heat content in the region show long-term warming trends larger than the global average.

Glaciers with relatively long-term observations in the High Mountain Asia region experienced mass loss in the hydrological year 2019/2020, with an accelerating trend to date throughout the twenty-first century. The minimum sea-ice extent in 2020 was the second lowest since 1979.

Many parts of Regional Association II and the surrounding oceans experienced heat events in 2020. Temperatures reached 38.0 °C at Verkhoyansk on 20 June, provisionally the highest known temperature anywhere north of the Arctic Circle, and the Laptev Sea experienced a particularly intense marine heatwave from June to December concurrent with record low sea-ice extent and extreme atmospheric conditions.

An unusual wet spell in East Asia and heavy rainfall in South Asia during the Asian summer monsoon season, combined with frequent tropical cyclone activities, brought floods, landslides and associated socioeconomic impacts to the affected regions.

Cyclone Amphan, one of the strongest cyclones ever recorded, hit densely populated coastal areas in Bangladesh and India during the rapid spread of COVID-19 in May 2020. The response to the impact of Amphan was made difficult owing to restrictions imposed during the pandemic and the disruption of supply chains.

In 2020 floods and storms affected approximately 50 million people, including over 5 000 lives lost in the region. Climate and weather events had major and diverse impacts on population movements and on the vulnerability of people on the move in Asia throughout the year.

The coronavirus (COVID-19) pandemic complicated disaster management efforts and countries faced the dual challenge of tackling the pandemic and climate-related hazards.

Supporting resilient recovery from the pandemic and the achievement of the 2030 Agenda for Sustainable Development requires a better understanding of risks, investment in renewable energy and frontier technologies, health, environment, and social protection, and ensuring targeted and forward-looking fiscal spending.

It is essential to adapt and build resilience to climate variability and change and to extreme climate events, especially in high-risk and low-capacity parts of the region. The Global Framework for Climate Services provides guidance on the implementation of operational systems and services needed to support adaptation and resilience development projects and programmes that respond to the priorities identified by Parties in their Nationally Determined Contributions to the Paris Agreement.

PART I – PHYSICAL ASPECTS

1.1 HIGHLIGHTS OF GLOBAL CLIMATE INDICATORS

- Concentrations of the major greenhouse gases, carbon dioxide (CO_2), methane (CH_4) and nitrous oxide (N_2O), continued to increase and reached record highs despite the temporary reduction in emissions in 2020 related to measures taken in response to COVID-19.

- The year 2020 was one of the three warmest years on record. The past six years, including 2020, have been the six warmest years on record. Temperatures reached 38.0 °C at Verkhoyansk, Russian Federation, on 20 June, provisionally the highest recorded temperature anywhere north of the Arctic Circle.

- Sea-level rise is accelerating. In addition, ocean heat storage and acidification continue to increase.

- The Arctic minimum sea-ice extent in September 2020 was the second lowest in the 42-year satellite record.

- The trend of Antarctic ice sheet mass loss accelerated around 2005, and currently, Antarctica loses approximately 175 to 225 gigatons (Gt) of ice per year.

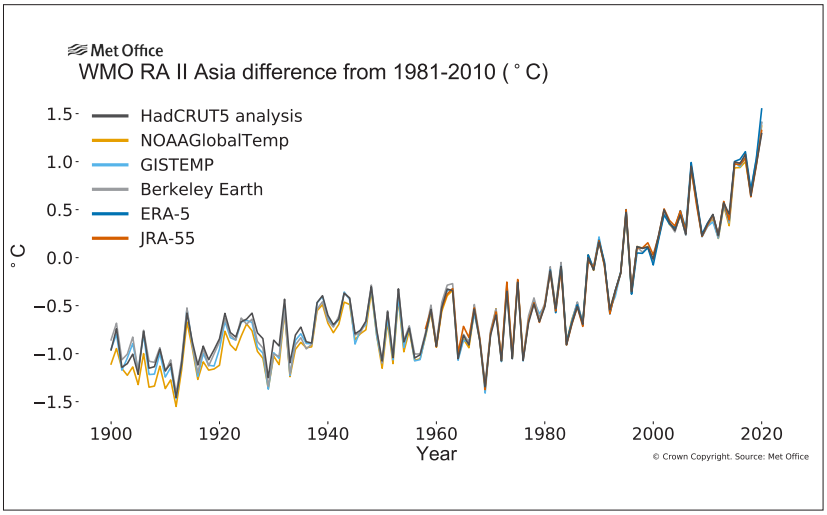

Figure 1. Annual mean temperature anomalies 1900–2020 (°C) averaged over Asia, relative to the 1981–2010, for six global temperature data sets as indicated in the legend. *Source:* MetOffice, UK. *Note:* HadCRUT, Berkeley Earth, NOAAGlobalTemp and GISTEMP are based on in situ observations. ERA5 and JRA-55 are reanalysis data sets. For details of the data sets and plotting, see Temperature data at the end of this report.

1.2 KEY INDICATORS OF CLIMATE IN ASIA FOR 2020 AND THEIR LONG-TERM TRENDS

1.2.1 TEMPERATURE

Temperature at Earth's surface, in conjunction with precipitation, has a great impact on natural systems and on humans.

In 2020, the mean temperature over Asia[1] was 1.39 °C above the 1981–2010 average, which places 2020 as the warmest year on record in all data sets used for this assessment. The spread of the estimates ranges between 1.29 °C and 1.55 °C (Figure 1). Although the overall warmth of 2020 is clear, there were variations in temperature anomalies across the region (Figure 2). In most land areas of the region, temperatures were warmer than average. In particular, Siberia had annual temperatures more than 5 °C above average near the Arctic Ocean coast, reflecting the exceptional warmth that persisted through most of the year in this area. Although above-average temperatures were dominant in 2020, some below-average temperatures were observed in Central and South Asia. For example, Kyrgyzstan experienced exceptionally cooler-than-normal conditions in autumn.

Over the long term, a warming trend has emerged since the latter half of the twentieth century in Asia, as indicated in Figures 1 and 3. In the two recent sub-periods (1961–1990 and 1991–2020), the warming trends in Asia, which has the largest land mass expanding to the polar region, have exceeded the global mean value. As stated in the Intergovernmental Panel on Climate Change (IPCC) special report on climate change and land,[2] this could reflect that the observed mean land surface air temperature in Asia has risen considerably more than the global mean (land and ocean) surface temperature and that the Arctic land surface temperatures have substantially increased over the past 50 years.

1 WMO Regional Association for Asia (RA II) geographical domain definition in Figure 2.

2 IPCC, 2019a: *Climate Change and Land: an IPCC Special Report on Climate Change, Desertification, Land Degradation, Sustainable Land Management, Food Security, and Greenhouse Gas Fluxes in Terrestrial Ecosystems* (P.R. Shukla et al., eds.), https://www.ipcc.ch/srccl/.

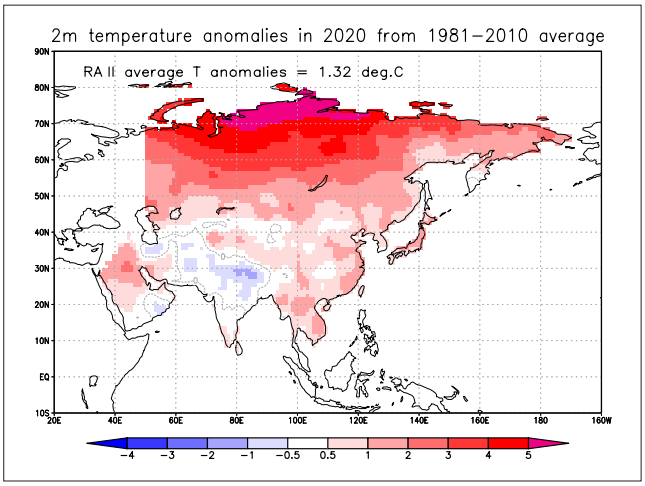

Figure 2. Temperature anomalies (°C) relative to the 1981–2010 long-term average from the JRA-55 reanalysis for 2020.
Source: Tokyo Climate Center, Japan Meteorological Agency

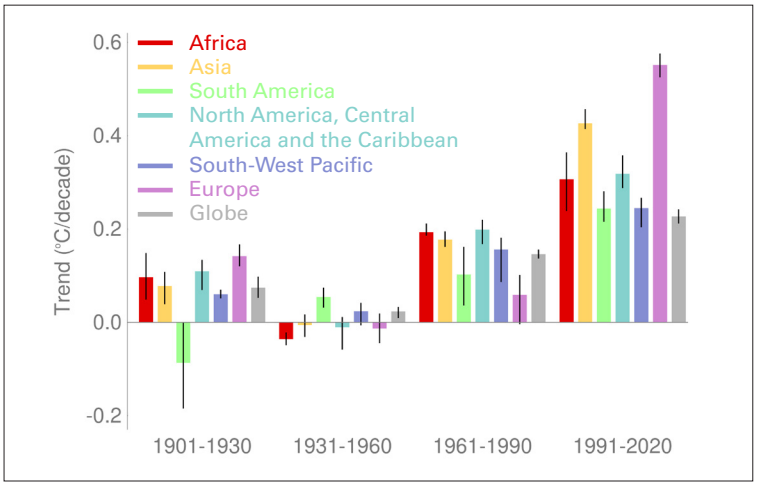

Figure 3. Trends in mean surface air temperature for the six WMO Regions and the global mean (°C) over four sub-periods using the six data sets (see Figure 1). The bars indicate the trend in the mean of the data sets. The black lines indicate the range between the largest and the smallest trends in the individual data sets.

1.2.2 PRECIPITATION

Precipitation is a key climate parameter, closely related to indispensable resources for human activities (e.g. water for drinking and domestic purposes, agriculture and hydropower). It also drives major climatic events such as droughts and floods. In 2020, the largest absolute precipitation excesses, with roughly 1 000 mm/yr, were found in eastern Asia and on the north-east coast of the Arabian Sea. The largest relative anomalies of total annual precipitation relative to the 1981–2010 average were found in these regions: from western to central Siberia, the western Arctic coast of Asia, the eastern part of East Asia, from western India to Pakistan, and the south-eastern Arabian Peninsula. The lowest relative precipitation anomalies were found in the Arabian Peninsula and Mesopotamia, in the Central Asian mountains, and around the Caspian Sea and North-East Asia (Figure 4). Based on time series analyses of the area-mean annual precipitation totals from the GPCC data (see Precipitation data at the end of this report), 2020 was drier than normal in the western Asian steppe (region of 45°E–80°E, 40°N–55°N) and the South-East Asian monsoon region (but wetter than the previous year). In the polar regions (northward of 60°N), 2020 was wetter than normal; this was the fourth consecutive wetter-than-normal year. In the South-West Asia region that relies on winter precipitation, the annual total in 2020 was above normal, similar to the two previous years. Annual precipitation totals in the South and East Asian summer monsoon regions were above normal in 2020. While higher annual totals were observed for the South Asian monsoon region (see also Asian summer monsoon under 1.2.6), the amounts in the East Asian summer monsoon region were also relatively high, as indicated by the annual precipitation percentage of 190%–200% in maximums.

1.2.3 SEA-SURFACE TEMPERATURE AND OCEAN HEAT CONTENT

Sea-surface temperature

Sea-surface temperature (SST) is an important physical indicator of Earth's climate system. Changes in SSTs directly affect the ocean-atmosphere coupling by altering the energy, momentum and gas exchanges between the two Earth system components,[3] thereby affecting regional and global circulation. Changes in SSTs also critically affect marine ecosystems.[4]

3 IPCC, 2019b: *IPCC Special Report on the Ocean and Cryosphere in a Changing Climate* (H.-O. Pörtner et al., eds.), https://www.ipcc.ch/srocc/.

4 Lehodey, P. et al., 2006: Climate variability, fish, and fisheries. *Journal of Climate*, 19(20): 5009–5030, https://doi.org/10.1175/JCLI3898.1.

The sea surface shows an overall warming trend in the Asian oceanic area, with the largest rates of more than 0.04 °C/yr in the areas of the Kuroshio Current system, the Arabian Sea, the southern Barents Sea and Kara Sea, and the south-eastern Laptev Sea (Figure 5, left). This is about three times the global surface ocean warming rate of 0.015 ± 0.001 °C per year.[5] In 2020, the area-averaged SST anomalies reached record high values in the Indian Ocean (>0.5 °C), the Pacific Ocean (>0.6 °C) and the Arctic Ocean (>0.6 °C) (Figure 5, right).

The Barents Sea is identified as a climate change hotspot[6] and a gateway for the recent Arctic amplification linked to rapid climate change.[7] Surface ocean warming in this area also has a major impact on the observed sea-ice loss,[8] a positive feedback mechanism which further enhances ocean warming.[9,10] For example, enhanced ocean warming in the Kara Sea has been linked to the sea-ice loss in this area.[11] In conjunction with the Siberian heatwave,[12] ocean warming has led to a record sea-ice loss in the Laptev Sea in 2020[13] (see also 1.3.2 - Heatwaves and warm spells).

5 Copernicus Marine Environment Monitoring Service, 2021: Global ocean anomaly time series of sea surface temperature, https://marine.copernicus.eu/access-data/ocean-monitoring-indicators/global-ocean-anomaly-time-series-sea-surface-temperature.

6 Schlichtholz, P., 2019: Subsurface ocean flywheel of coupled climate variability in the Barents Sea hotspot of global warming. *Scientific Reports*, 9: 13692, https://doi.org/10.1038/s41598-019-49965-6.

7 Dai, A. et al., 2019: Arctic amplification is caused by sea-ice loss under increasing CO_2. Nature Communications, 10: 121, https://doi.org/10.1038/s41467-018-07954-9.

8 Aobe, S. et al., 2021: Section 4.1: Sea-ice and ocean conditions surprisingly normal in the Svalbard-Barents Sea region after large sea-ice inflows in 2019. In: *Copernicus Marine Service Ocean State Report*. Issue 5, Journal of Operational Oceanography (forthcoming).

9 Kumar, A. et al., 2021: Spatio-temporal change and variability of Barents-Kara sea ice, in the Arctic: ocean and atmospheric implications. *Science of the Total Environment*, 753: 142046, https://doi.org/https://doi.org/10.1016/j.scitotenv.2020.142046.

10 IPCC, 2019b: *IPCC Special Report on the Ocean and Cryosphere in a Changing Climate*.

11 Kohnemann, S.H.E. et al., 2017: Extreme warming in the Kara Sea and Barents Sea during the winter period 2000–16. *Journal of Climate*, 30(22): 8913–8927, https://doi.org/10.1175/JCLI-D-16-0693.1.

12 Allen, M., 2021: Siberian heat wave nearly impossible without human influence. *Eos*, 102, 17 June, https://doi.org/10.1029/2021EO159771.

13 National Snow and Ice Data Center, 2020: Laptev Sea lapping up the heat in June, 2 July, http://nsidc.org/arcticseaicenews/2020/07/laptev-sea-lapping-up-the-heat-in-june/.

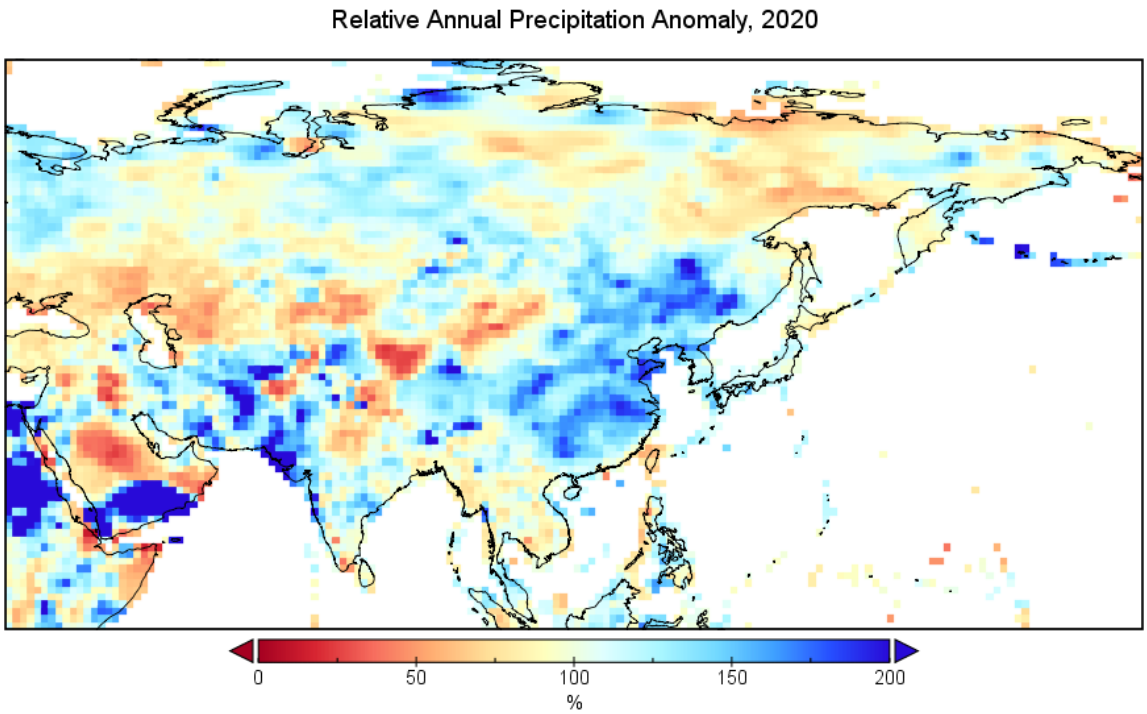

Figure 4. Precipitation anomalies for 2020, expressed as a percentage of the 1981–2010 average. *Source:* Global Precipitation Climatology Centre (GPCC), Deutscher Wetterdienst, Germany

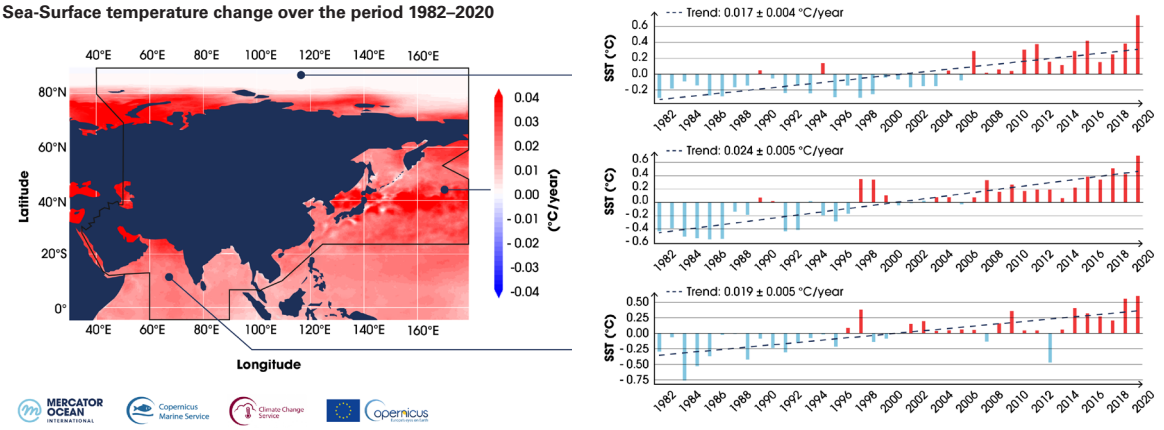

Figure 5. Left: Trends of SST (°C per year) over the period 1982–2020 derived from the remote sensing product (*SST_GLO_SST_L4_REP_OBSERVATIONS_010_024*) downloaded from Copernicus Marine Service. Right: Area-averaged time series of SST anomalies (°C) relative to the 1982–2020 reference period for three areas indicated (see left): the entire Pacific area; the entire Indian Ocean area; and the area north of 60°N (the Arctic). For each area, the linear trend over the full period is indicated by grey dashed lines.

Ocean heat content

More than 90% of the excess heat in the climate system due to human activities is absorbed and stored by the ocean, leading to an increase in the ocean heat content (OHC) and the warming of the ocean.[14,15] Ocean warming contributes to about 40% of the observed global mean sea-level rise.[16,17] Moreover, it alters ocean currents and, indirectly, storm tracks.[18,19,20] Lastly, it increases ocean stratification[21] and can lead to changes in marine ecosystems.[22,23,24,25]

Since 1993, most of the oceanic areas in the region have recorded an upward trend in OHC at the upper layer of the ocean (0–700 m). The upward trend is particularly strong in the Arabian Sea and in the Kuroshio Current regime, with rates exceeding 2 watts per square metre (W/m^2) (Figure 6, left). This is more than three times faster than the global mean upper-ocean warming rate of 0.6 W/m^2 over the same period.[26] In 2020, the area-averaged surface ocean warming reached record values in the Asia Pacific. Subsurface warming (0–700 m) in the Indian Ocean area amounts to 0.7 ± 0.2 W/m^2 on average, which is due to the concurrent influences of anthropogenic forcing and climate variability.[27] North of 60°N, the OHC trend is not significant and is dominated by interannual variations (Figure 6, right).

14 IPCC, 2019b: *IPCC Special Report on the Ocean and Cryosphere in a Changing Climate*.

15 von Schuckmann, K. et al., 2020: Heat stored in the Earth system: Where does the energy go? *Earth System Science Data*, 12(3): 2013–2041, https://doi.org/10.5194/essd-12-2013-2020.

16 Oppenheimer, M. et al., 2019: Sea level rise and implications for low-lying islands, coasts and communities. In: *IPCC Special Report on the Ocean and Cryosphere in a Changing Climate* (H.-O. Pörtner et al., eds.), https://www.ipcc.ch/srocc/.

17 World Climate Research Programme (WCRP) Global Sea Level Budget Group, 2018: Global sea-level budget 1993–present. *Earth System Science Data*, 10(3): 1551–1590, https://doi.org/10.5194/essd-10-1551-2018.

18 IPCC, 2018: *Global Warming of 1.5°C: an IPCC Special Report on the Impacts of Global Warming of 1.5°C above Pre-industrial Levels and Related Global Greenhouse Gas Emission Pathways, in the Context of Strengthening the Global Response to the Threat of Climate Change, Sustainable Development, and Efforts to Eradicate Poverty* (V. Masson-Delmotte et al., eds.), https://www.ipcc.ch/sr15/.

19 Woollings, T. et al., 2012: Response of the North Atlantic storm track to climate change shaped by ocean–atmosphere coupling. *Nature Geoscience*, 5: 313–317, https://doi.org/10.1038/ngeo1438.

20 Yang, H. et al., 2016: Intensification and poleward shift of subtropical western boundary currents in a warming climate. *Journal of Geophysical Research: Oceans*, 121(7): 4928–4945, https://doi.org/10.1002/2015JC011513.

21 Li, G. et al., 2020. Increasing ocean stratification over the past half-century. *Nature Climate Change*, 10: 1116–1123, https://doi.org/10.1038/s41558-020-00918-2.

22 García Molinos, J. et al., 2016: Climate velocity and the future global redistribution of marine biodiversity. *Nature Climate Change*, 6: 83–88, https://doi.org/10.1038/nclimate2769.

23 Gattuso, J.-P. et al., 2015: Contrasting futures for ocean and society from different anthropogenic CO_2 emissions scenarios. Science, 349(6243): aac4722, https://doi.org/10.1126/science.aac4722.

24 IPCC, 2019a: *Climate Change and Land*.

25 Ramírez, F. et al., 2017: Climate impacts on global hot spots of marine biodiversity. *Science Advances*, 3(2): e1601198, https://doi.org/10.1126/sciadv.1601198.

26 von Schuckmann et al., 2020: Heat stored in the Earth system: Where does the energy go?

27 Li, Y. et al., 2017: Enhanced decadal warming of the southeast Indian Ocean during the recent global surface warming slowdown. *Geophysical Research Letters*, 44(19): 9876–9884, https://doi.org/10.1002/2017GL075050.

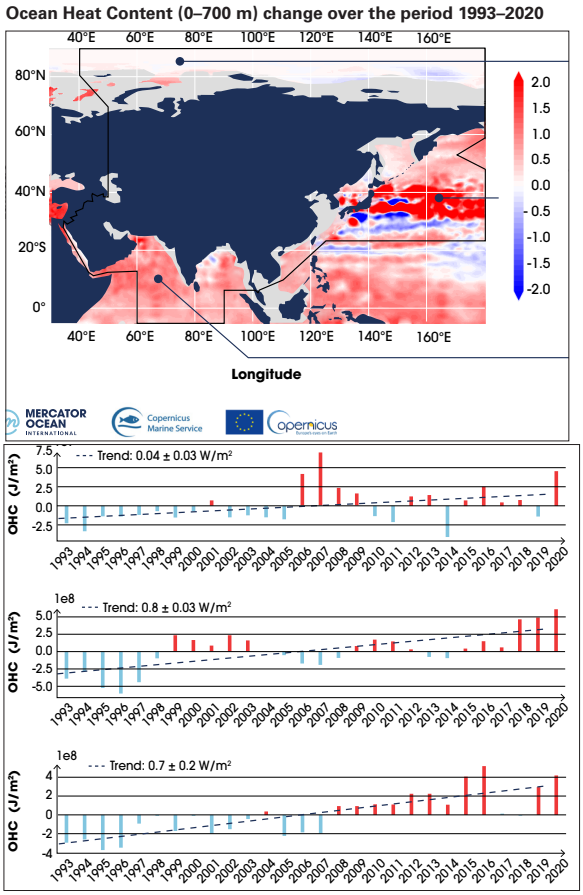

Figure 6. Left: Trends of OHC (W/m^2) over the period 1993–2020, integrated from the surface down to 700 m depth and derived from the in situ-based product (*MULTIOBS_GLO_PHY_TSUV_3D_MYNRT_015_012*) downloaded from Copernicus Marine Service. Ocean warming rates at bathymetry shallower than 300 m have been excluded owing to product limitations linked to data sampling gaps (shown in grey). Right: Area-averaged time series of OHC anomalies (Joule per square metre (J/m^2)) relative to the 1993–2020 reference period for three areas indicated (see left): the entire Pacific area; the entire Indian Ocean area; and the area north of 60°N (the Arctic). For each area, the linear trend over the full period is indicated by grey dashed lines.

1.2.4 SEA LEVEL

Since the early 1990s, sea level has been routinely measured globally and regionally by a series of high-precision altimeter satellites.[28] The data indicate that the global mean sea level has risen at an average rate of 3.3 ± 0.3 mm/yr and has accelerated during that time, in response to ocean warming and land-ice melt. They also show that the rate of rise varies geographically, mainly due to non-uniform ocean thermal expansion and regional salinity variations.[29,30,31]

Figure 7 shows the altimetry-based regional sea-level trends from January 1993 to June 2020 in the Indian and Pacific oceans, based on the Copernicus Climate Change Service (C3S) gridded sea-level product with 0.25° resolution. The map shows that in the North Indian Ocean (3.70 ± 0.1 mm/yr) and the Northwest Pacific Ocean (3.68 ± 0.1 mm/yr), the rates of sea-level rise are significantly higher than the global mean.

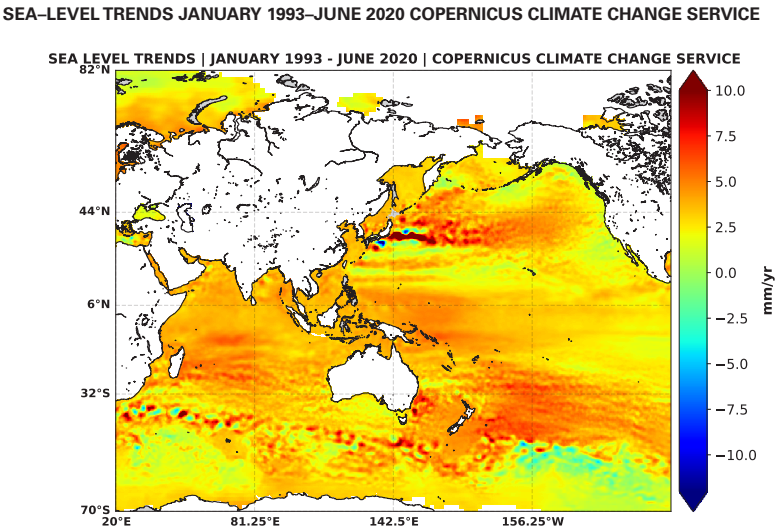

Figure 7. Spatial trend patterns in sea level (mm/yr) observed by altimeter satellites from 1993 to 2020. *Source:* C3S

28 In particular, Topex/Poseidon and its successors Jason-1, Jason-2, Jason-3 and Sentinel-6 MF launched in 1992, 2002, 2008, 2016 and 2020, respectively, as well as ERS-1 and ERS-2, Envisat, SARAL/Altika, and Sentinel-3A and Sentinel-3B.

29 Church, J.A. et al., 2013: Sea level change. In: *Climate Change 2013: the Physical Science Basis. Contribution of Working Group I to the Fifth Assessment Report of the Intergovernmental Panel on Climate Change* (T.F. Stocker et al., eds.). Cambridge and New York, Cambridge University Press, https://www.ipcc.ch/report/ar5/wg1/.

30 Cazenave, A. et al., 2018: Contemporary sea level changes from satellite altimetry: What have we learned? What are the new challenges? *Advances in Space Research*, 62(7): 1639–1653, https://doi.org/10.1016/j.asr.2018.07.017.

31 Hamlington, B.D. et al., 2020: Understanding of contemporary regional sea-level change and the implications for the future. *Reviews of Geophysics*, 58(3): e2019RG000672, https://doi.org/10.1029/2019RG000672.

1.2.5 CRYOSPHERE

The Arctic sea ice

Sea-ice extent is a key indicator of climate variability and the changes in the polar regions. The presence of sea ice strongly modulates surface ocean waves and the air-sea exchanges of heat, momentum, moisture and gases to shape not only the regional climate but also the global climate.

The 15.1 million km^2 maximum sea-ice extent in the Arctic reached on 5 March 2020 was the eleventh lowest maximum sea-ice extent since 1979, with the maximum winter sea-ice extent observed in 1979 (16.77 million km^2).[32] Estimates of the sea-ice volume, which take into account depth as well as extent, based on numerical reanalysis, show that the 2020 sea-ice volume was similar to that of 2019, a year with one of the lowest sea-ice volumes on record. Similarly, maximum winter ice thickness observed at coastal stations was in general significantly thinner on the Siberian side of the Arctic (up to –50 cm for the Kara Sea).[33]

According to the consensus statement of the sixth session of the Arctic Climate Forum (ACF), the 3.9 million km^2 minimum sea-ice extent reached on 12 September 2020 was the second lowest minimum sea-ice extent since 1979, with the minimum summer sea-ice extent observed in 2012 (3.35 million km^2).[34] Other sources state that the Arctic minimum sea-ice extent observed on 15 September was 3.74 million km^2 and the minimum sea-ice extent in 2012 was 3.39 million km^2.[35] Estimates of the sea-ice volume based on numerical reanalysis show that the 2020 sea-ice volume was the second lowest, with 2012 and 2016 tied for the lowest.[36] The Arctic sea-ice cover in the summer of 2020 significantly differed in shape from that of 2019. The Eurasian shelf seas and the Northern Sea Route were completely ice free.[37] Ice conditions were not problematic for the entire Northern Sea Route during the spring and summer seasons of 2020 and significant incursions of old ice were not observed along the route during the 2020 summer season. For more information about the data sets, see Sea-ice data at the end of this report.

Glaciers

Glaciers react to climatic forcing at typical timescales of years to decades. Glacier changes are recognized as independent natural evidence of climate change. They affect global sea level, regional water cycles and local hazard situations.

High Mountain Asia is a high-elevation region centred on the Tibetan Plateau. It is home to approximately 100 000 km^2 of glaciers,[38] containing the largest volumes of ice outside of the polar regions. Moreover, the headwaters of 10 prominent Asian rivers are located in this area.

Glacier mass balance is an important indicator of glacier changes, which are controlled mainly by the mass and energy budget in response to changes in regional temperature, precipitation and surface radiation. According to the latest data from the World Glacier Monitoring Service (WGMS), in the hydrological year 2019/2020, global glaciers

---

32 Arctic Regional Climate Centre Network (ArcRCC-Network), 2020: *Arctic Climate Forum Consensus Statement: 2020 Arctic Summer Seasonal Climate Outlook (Along with a Summary of 2020 Arctic Winter Season)*. Fifth session of the Arctic Climate Forum (ACF), 27–28 May, https://arctic-rcc.org/sites/arctic-rcc.org/files/documents/acf-spring-2020/ACF-5_Consensus_Statement_final.pdf.

33 Ibid.

34 ArcRCC-Network, 2020: *Arctic Climate Forum Consensus Statement: 2020–2021 Arctic Winter Seasonal Climate Outlook (Along with a Summary of 2020 Arctic Summer Season)*. Sixth session of the ACF, 28–29 October, https://arctic-rcc.org/sites/arctic-rcc.org/files/documents/acf-fall-2020/ACF-6_Consensus_Statement_Final.pdf.

35 World Meteorological Organization (WMO), 2021: State of the Global Climate 2020 (WMO-No. 1264). Geneva.

36 ArcRCC-Network, 2020: 2020–2021 Arctic Winter Seasonal Climate Outlook. Sixth session of the ACF.

37 Ibid.

38 Yao, T. et al., 2019: Recent Third Pole's rapid warming accompanies cryospheric melt and water cycle intensification and interactions between monsoon and environment: multidisciplinary approach with observations, modeling, and analysis. *Bulletin of the American Meteorological Society*, 100 (3): 423–444, https://doi.org/10.1175/BAMS-D-17-0057.1.

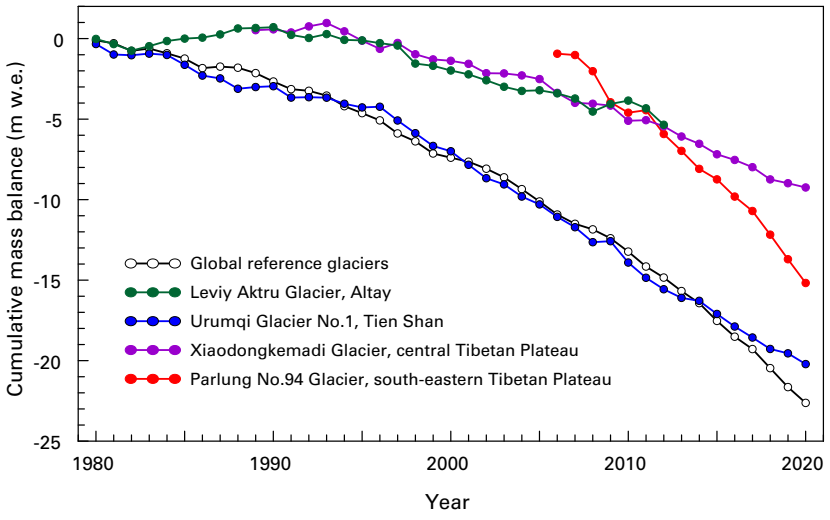

Figure 8. Cumulative mass changes (m w.e.) of four reference glaciers in the High Mountain Asia region and the average loss of global reference glaciers. Data sourced and updated from WGMS, 2021: Global Glacier Change Bulletin No. 4 (2018-2019) (M. Zemp et al., eds.). Zurich, WGMS, based on doi:10.5904/wgms-fog-2021-05; and Yao T. et al., 2012: Different glacier status with atmospheric circulations in Tibetan Plateau and surroundings. *Nature Climate Change*, 2: 663–667, https://doi.org/10.1038/nclimate1580.

continued to lose mass; in 2020, the global annual mass balance loss of reference glaciers with long-term observations was 0.982 metre water equivalent (m w.e.). In the past 40 years, all four glaciers with relatively long-term observations in the High Mountain Asia region experienced mass loss, with an accelerating trend in the twenty-first century (Figure 8). In particular, Parlung No. 94 in the south-eastern Tibetan Plateau (red line) shows larger cumulative mass loss than the average of the global reference glaciers (grey line) in the same period.

According to the preliminary results for 2019/2020, the reference glaciers observed in the High Mountain Asia region experienced regionally contrasting mass changes (Figure 9). While most glaciers in western Tien Shan and Pamir Alai (Kyrgyzstan) were close to balanced-budget conditions (meaning a small gain or loss of ice), other glaciers overall underwent high mass losses, with the mass balance in 2019/2020 of –1.476 m w.e. for Parlung No. 94 (China) in the south-eastern Tibetan Plateau and –2.784 m w.e. for Thana (Bhutan) in the eastern Himalayas, which were well beyond the annual mean mass loss of global reference glaciers.

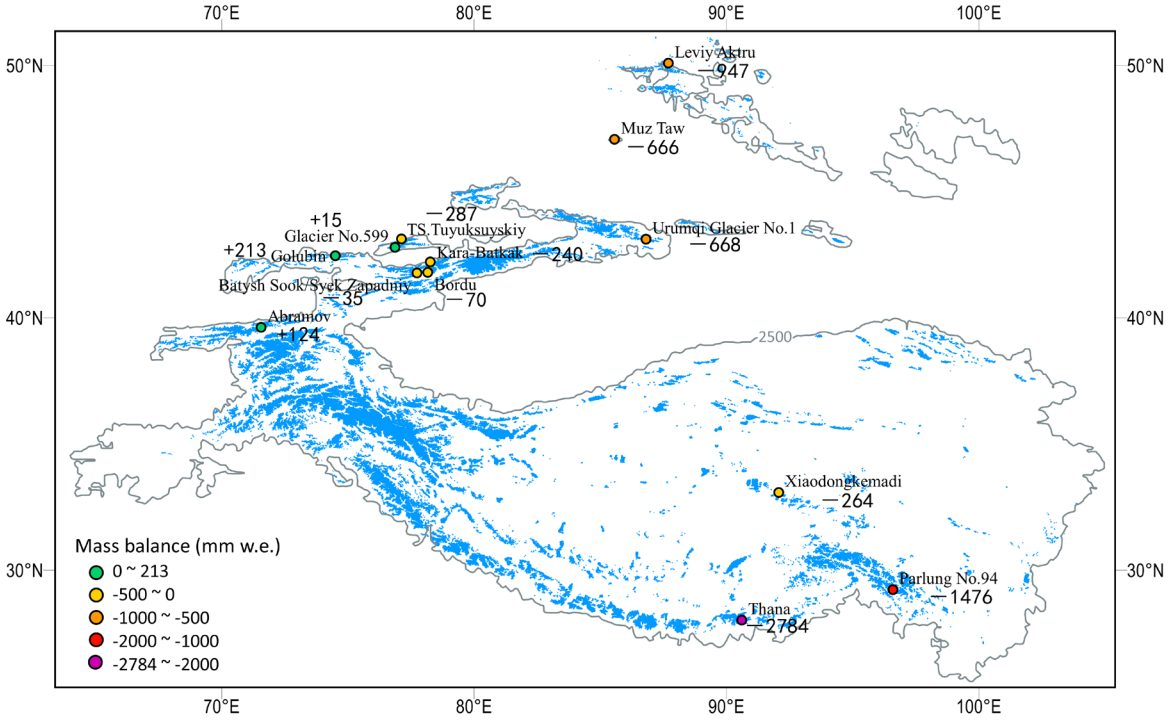

Figure 9. Preliminary estimations of 2019/2020 mass balance of glaciers in the High Mountain Asia region, with the area highlighted with grey contours at 2 500 metres above sea level. Note: Region extent is depicted on Figure 11. *Sources*: WMO Third Pole Regional Climate Centre Network (TPRCC-Network); WGMS (the original investigators from Bhutan, China, Kazakhstan, Kyrgyzstan and Russian Federation).

Snow cover

Snow cover plays an important role in feedback mechanisms in the climate system (e.g. albedo, run-off, soil moisture and vegetation) and is hence crucial for monitoring climate change. In the past 24 years, spring (March to May) snow cover extent (SCE) over Asia exhibited decadal variations. The main characteristic of this variations includes above normal anomalies before 2006 and dominant below normal anomalies thereafter. In the spring of 2020, SCE in Asia was about 14.0 million km^2, 0.7 million km^2 less than the 1998–2020 mean, which continued the dominant feature of below-normal SCE since the mid-2000s (Figure 10).

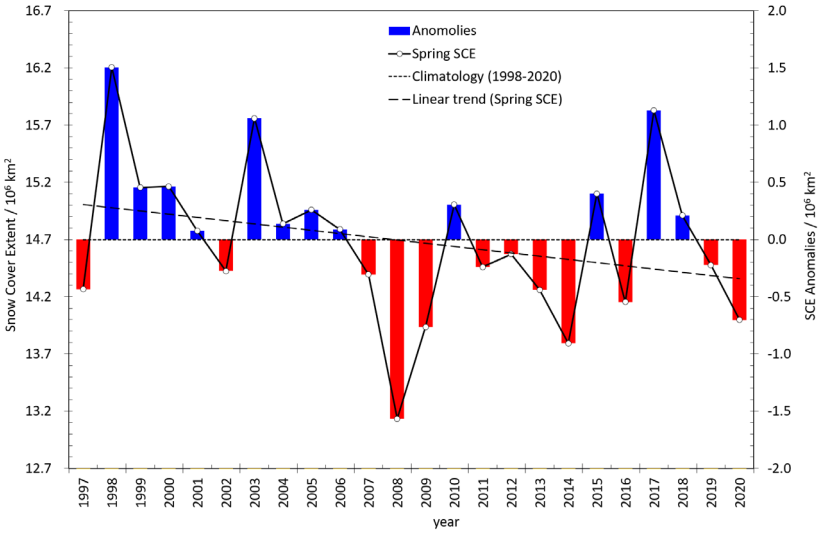

Figure 10. SCE in Asia (left axis) and anomalies in blue and red (right axis) in the spring of 1997–2020. The dotted line denotes the climatology mean 1998–2020. The dashed line denotes the linear trend 1997–2020. Data sourced from the Interactive Multisensor Snow and Ice Mapping System.

Spatially, mean SCE[39] in the spring of 2020 was the largest in the high mountain areas of Asia, while it was the smallest along the south edge of the high-latitude plain and in the central Tibetan Plateau (Figure 11). Compared with the climatology mean from 1998 to 2020, SCE in the spring of 2020 was about 5–120 km^2 below normal in most of northern Asia (i.e. north of 40°N). In some areas, including Tien Shan and the Altay Mountains, it was 120 km^2 below normal or less. However, in the high mountain areas of its eastern part – including the Stanovoy Range, the Greater Xing'an Mountains, the Xiaoxing'an Mountains and the Changbai Mountains – it was 5–60 km^2 above normal. In the region south of 40°N, SCE was dominantly above normal except in the Kunlun Mountains, with 30–120 km^2 above normal in the mid-eastern Tibetan Plateau and the middle Himalayas. In some areas, it was more than 120 km^2 above normal.

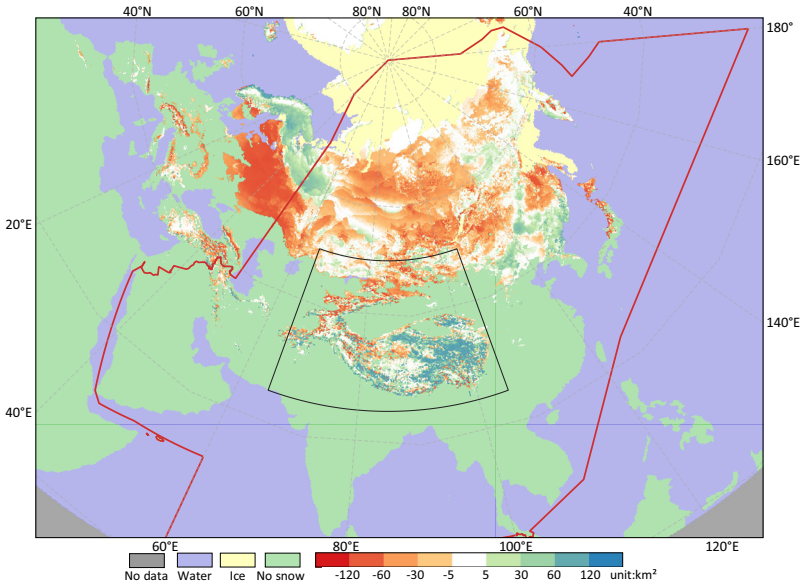

Figure 11. Anomalies of mean SCE in the spring of 2020, relative to 1998–2020. Note: The red line delimits the Asia mean SCE calculation extent. The black line marks the extent of Figure 9 High Mountain Asia region. *Source:* The Interactive Multisensor Snow and Ice Mapping System.

39 Monthly snow cover extent (SCE) is obtained by dividing the number of monthly snow cover days of each grid point by the total number of days in that month, and then multiplying by the area of the grid. The mean SCE in spring is the average of SCE in March, April and May. The Asia mean SCE is obtained by averaging SCE of all grids within the area bounded by the red line on Figure 11.

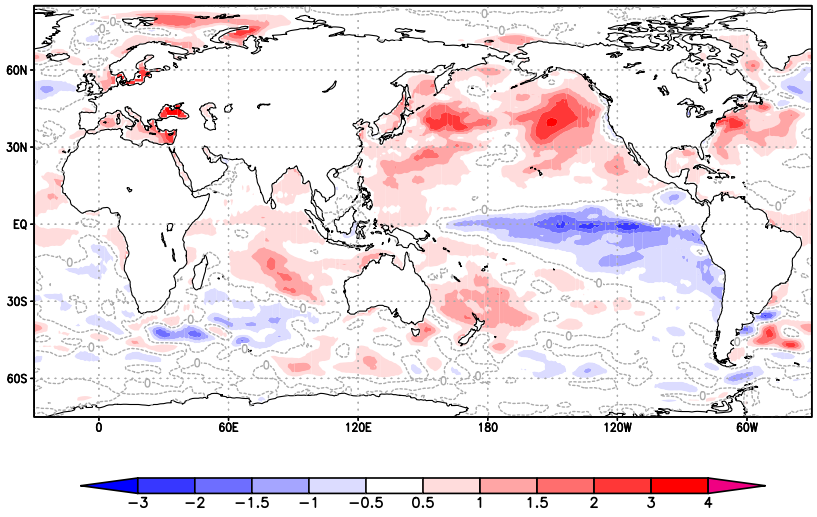

Figure 12. Global SST anomalies (°C) in November 2020. Anomalies are defined as deviations from the 1981–2010 mean. *Source:* Tokyo Climate Center, Japan Meteorological Agency

1.2.6 MAJOR DRIVERS OF CLIMATE VARIABILITY IN THE REGION

There are many modes of natural variability, often referred to as climate patterns or climate modes, which affect weather at timescales ranging from days to months or even decades. Surface temperatures change relatively slowly over the ocean, so recurring SST patterns can be used to understand and, in some cases, predict the more rapidly changing patterns of weather over land on seasonal timescales. Similarly, albeit at a faster rate, known pressure changes in the atmosphere can help explain certain regional weather patterns.

El Niño–Southern Oscillation

In Asia, the El Niño–Southern Oscillation is one of the most important drivers of year-to-year variability in weather patterns.[40] El Niño, characterized by higher-than-average SSTs in the eastern Pacific accompanying a weakening of the trade winds, typically has a warming influence on global temperatures. La Niña, characterized by below-average SSTs in the central and eastern Pacific and a strengthening of the trade winds, has the opposite effect. For example, East Asia tends to experience warmer-than-normal winters under the El Niño condition, and vice versa.

From the beginning of 2020 to the boreal spring, SSTs in the El Niño monitoring region were near the relevant climatological averages. In the summer, La Niña developed and intensified through the northern hemisphere autumn into a moderate strength through the rest of 2020 (Figure 12). The atmospheric circulation responded to the anomalous oceanic conditions and induced convective activity that led to anomalous climate conditions over Asia. The heavy rainfall over mainland South-East Asia in October and November and the persistent South Asian summer monsoon and heavy rainfall in September and October was a typical response to this La Niña event, which brought warmer SSTs around these areas and enhanced active convection.

Indian Ocean Dipole and Indian Ocean Basin Mode

The Indian Ocean Dipole (IOD) is an inherent and major mode of climate variability over the Indian Ocean. It is characterized by SST anomalies and associated convective anomalies with opposite signs in the eastern and western tropical Indian Ocean. In the positive IOD phase, below-normal SSTs and suppressed convective activity are seen in the south-eastern part of the tropical Indian Ocean, while SSTs in the western tropical Indian Ocean are above normal with enhanced convection. Negative IOD events have anomalies with signs opposite to those of its positive phase. An unusually strong positive IOD took place in 2019, with the Dipole Mode Index peaking at 2.1 °C in October, the highest on record.[41] Following the significant Indian Ocean basin warming in September 2019, the Indian Ocean Basin Mode (characterized by basin-wide warming or cooling) index reached 1.53 of its detrended standard deviation in June–July 2020, which was the third-highest value since

40 Tokyo Climate Center. Impacts of El Niño/La Niña and Indian Ocean Dipole events on the global climate, http://ds.data.jma.go.jp/tcc/tcc/products/climate/ENSO/index.htm.

41 Doi, T. et al., 2020: Predictability of the super IOD event in 2019 and its link with El Niño modoki. *Geophysical Research Letters*, 47(7): e2019GL086713, https://doi.org/10.1029/2019GL086713.

records began in 1961.[42] The strong positive IOD event in 2019 and the significant Indian Ocean Basin Mode warming in the summer of 2020 were important contributors to the extreme Yangtze River flooding in 2020.[43,44] The residual influence of the positive IOD in the summer and autumn of 2019, namely higher SSTs in the northern Indian Ocean, might be related to the hot conditions over southern India and Sri Lanka in January and February 2020.

Arctic Oscillation and winter monsoon

The Arctic Oscillation (AO) is a large-scale atmospheric pattern that influences weather throughout the northern hemisphere.[45] The positive phase is characterized by below-normal mean sea-level pressure over the Arctic and above-normal mean sea-level pressure over the northern Pacific and Atlantic oceans. During the positive AO phase, the polar jet stream is more zonal and located farther north than average, locking up cold Arctic air; storms can be shifted northward of their usual paths. The mid-latitudes of Siberia and East Asia generally see fewer cold air outbreaks than normal during the positive AO phase. A negative AO has the opposite effect and is associated with a more meandering jet stream and cold air spilling south into the mid-latitudes. In the 2019/2020 winter, a strong positive AO event (the second strongest on record), with a weaker and smaller Siberian High, brought significantly warmer-than-normal conditions over Siberia, Central Asia and East Asia.[46]

Asian summer monsoon

The Asian monsoon is one of Earth's most energetic weather events, which influences the global atmospheric circulation.[47] It is also a key driver of the seasonal changes in atmospheric circulation and precipitation (dry and wet seasons) over several countries in South and East Asia. In particular, precipitation associated with the Asian summer monsoon is a key source of fresh water in those regions. In 2020, the first entry of the South Asian summer monsoon over the region took place on 17 May, over the southern Bay of Bengal, the Nicobar Islands and the Andaman Sea. However, the monsoon did not advance further for about nine days. After this long hiatus, during 27–29 May, the monsoon progressed over the entire Andaman Sea, the Andaman and Nicobar Islands, more parts of the southern Bay of Bengal, southern Sri Lanka, some parts of the south-western and south-eastern Arabian Sea and the Maldives-Comorin area. Subsequently, it progressed further northward and set over the southern tip of India on its normal date of 1 June. Most parts of South Asia were covered by the summer monsoon by the end of June, well ahead of its normal date of 8 July.[48] The area-weighted rainfall over India during the 2020 summer monsoon season was above normal (see also 1.2.2 - Precipitation), as it was in 2019 after five years of below-normal monsoon rainfall (Figure 13). Normal to above-normal rainfall was recorded during the summer monsoon season (June–September) over most parts of the region. Pakistan and Sri Lanka reported much-above-normal country-averaged rainfall during the summer monsoon season.

---

42 Ding, Y. et al., 2021: The record-breaking Meiyu in 2020 and associated atmospheric circulation and tropical SST anomalies. *Advances in Atmospheric Sciences*, https://doi.org/10.1007/s00376-021-0361-2.

43 Takaya, Y. et al., 2020: Enhanced Meiyu-Baiu rainfall in early summer 2020: aftermath of the 2019 super IOD event. *Geophysical Research Letters*, 47(22): e2020GL090671, https://doi.org/10.1029/2020GL090671.

44 Zhou, Z.-Q. et al., 2021: Historic Yangtze flooding of 2020 tied to extreme Indian Ocean conditions. *Proceedings of the National Academy of Sciences of the United States of America*, 118(12): e2022255118, https://doi.org/10.1073/pnas.2022255118.

45 Deser, C., 2000: On the teleconnectivity of the "Arctic oscillation". *Geophysical Research Letters*, 27(6): 779–782, https://doi.org/10.1029/1999GL010945.

46 Kryjov, V.N., 2021: Climate extremes of the 2019/2020 winter in northern Eurasia: contributions by the climate trend and interannual variability related to the Arctic Oscillation. *Russian Meteorology and Hydrology*, 46: 61–68.

47 Trenberth, K.E. et al., 2000: The global monsoon as seen through the divergent atmospheric circulation. *Journal of Climate*, 13(22): 3969–3993, https://doi.org/10.1175/1520-0442(2000)013<3969:TGMAST>2.0.CO;2.

48 Pai, D.S. et al., 2020, Normal dates of onset/progress and withdrawal of southwest monsoon over India. *MAUSAM*, 71(4): 553–570, https://mausamjournal.imd.gov.in/index.php/MAUSAM/article/view/33.

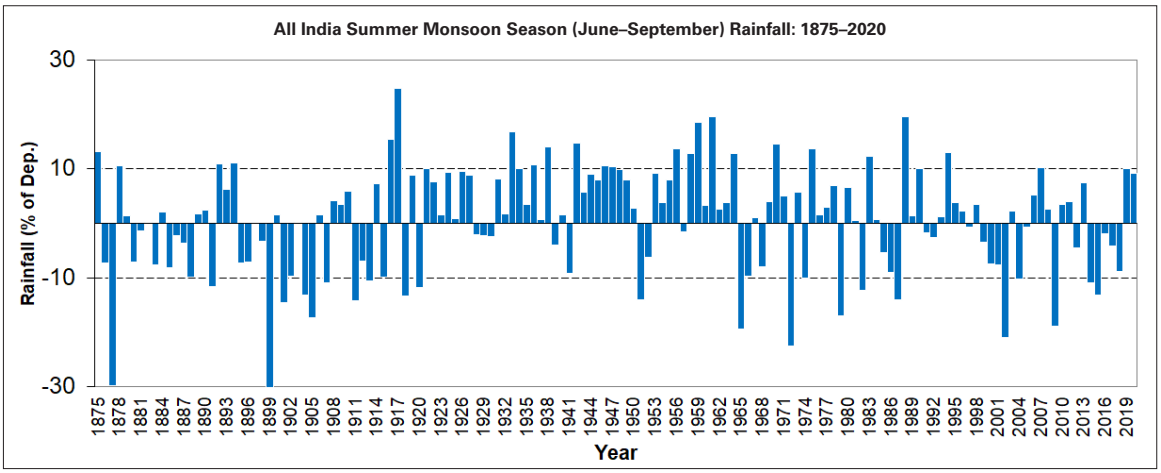

Figure 13. Time series of area-weighted rainfall anomalies over India (representative of South Asia) in the summer monsoon season (June–September) for the period 1875–2020. Climatology is the 1961–2010 average. *Source:* Regional Climate Centre, Pune

1.3 EXTREME EVENTS

1.3.1 EXTREME RAINFALL AND FLOODS

With regard to extremes based on daily precipitation totals, the highest daily 5-day sum and the 95th percentile of daily precipitation totals were observed in the Asian monsoon region and the western part of Asia (Figure 14).

An unusual wet spell persisted in the summer over the regions from the Yangtze River basin to the Republic of Korea to western and eastern Japan, associated with the persistent East Asian summer monsoon. It brought moist air to those regions and caused exceptionally strong and prolonged precipitation along the Meiyu/Baiu/Changma front in June–July 2020. In China, the cumulative monsoon rainfall over the affected region was the highest since records began in 1961. In Japan and the Republic of Korea, floods during this wet spell brought tens of casualties in each country (see also 2.1.1 - Affected populations and damage and 2.1.3 - Agriculture and food security).

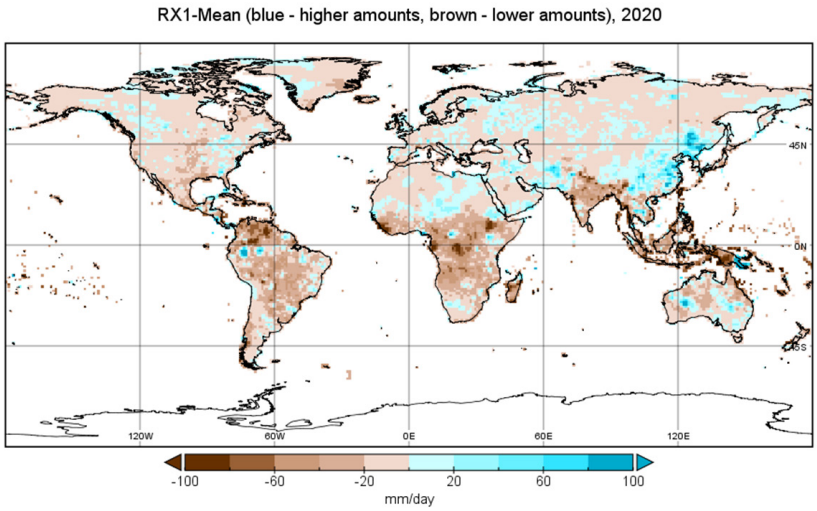

Figure 14. Anomalies (mm/day) of the highest daily precipitation totals. Blue indicates more extreme daily precipitation than the long-term mean, and brown indicates less extreme daily precipitation than the long-term mean. Note: The climatology period used here is the full length of the global daily precipitation data set. *Source:* GPCC, Deutscher Wetterdienst, Germany

During the summer monsoon season in 2020, countries in South Asia suffered from heavy rainfall and the resulting floods and landslides. Pakistan experienced the wettest August on record since 1961. The total rainfall in Karachi was particularly notable: Karachi-Faisal recorded 588.0 mm for August, the highest August precipitation on record for this observation station, and 231.0 mm of rainfall on 28 August, which was the heaviest daily rainfall on record for this station. As a result of the unprecedented August rainfall, one of the country's most devastating urban flooding events occurred in the metropolis of Karachi, affecting millions of people and inflicting widespread infrastructure damage (Figure 15, top) (see also 2.1.1 - Affected populations and damage). Heavy rainfall and flood-related incidents reportedly claimed hundreds of lives from parts of India over various seasons of the year.[49] Nepal experienced some flood events during July and September. During 8–10 July, associated with the shifting of the monsoon trough north of its normal position, widespread rainfall was experienced

49 United Nations Office for the Coordination of Humanitarian Affairs (OCHA), Humanitarian Response, 2020: India: floods and landslides – Jul 2020, https://www.humanitarianresponse.info/en/disaster/fl-2020-000164-ind.

Figure 15. Top row: Karachi floods in 2020. Bottom row: Floods in Myanmar. *Sources*: Pakistan Meteorological Department; Department of Meteorology and Hydrology, Myanmar

over central and northern parts of Nepal in and around Sindhupalchowk district, causing flooding and landslides that resulted in the loss of lives and property.

Owing to heavy rainfall events during July and August, water levels in the Ayeyarwady, Thanlwin and Chindwin rivers in Myanmar rose significantly, causing floods in several areas along the riverbanks and displacing thousands of people from the areas (Figure 15, bottom). Over 160 casualties were reported after a massive landslide in a jade mine in Kachin state on 2 July. Also in Kachin state, close to 4 000 people were displaced in the townships of Myitkyina and Hpakant on 27–28 September following heavy monsoon rains and floods.[50]

In October, continuous impacts of the combination of tropical cyclones and north-east monsoon caused the monthly total rainfall of two to four times higher than monthly average. In addition, some locations in the north and the middle of central Viet Nam recorded historical daily rainfall such as A Luoi (Thua Thien Hue) 594 mm on the 10th, Khe Sanh (Quang Tri) 582 mm on the 16th, Ba Don (Quang Binh) 756 mm and Hoanh Son (Ha Tinh) 302 mm on the 19th.

In December, a mid-latitude cyclone triggered heavy rainfall in the region over the western windward faces of the Zagros Mountains in the south-western part of the Islamic Republic of Iran. Heavy rains and flooding in upper-mountain areas inundated many parts of the Khuzestan Province along the Karoon River in the plains and lowlands of the south-west of the Islamic Republic of Iran.

1.3.2 HEATWAVES AND WARM SPELLS

Many parts of the region experienced heat events in 2020. Temperatures over the Asian part of Russia were exceptionally high from January to November. Temperatures reached 38.0 °C at Verkhoyansk (67.57°N, altitude of 135 m) on 20 June, provisionally the highest known temperature anywhere north of the Arctic Circle (66.3°N). The main feature of the circulation in the Arctic region in the summer season was the intense stable anticyclones

50 OCHA, ReliefWeb, 2020: Myanmar: floods and landslides - Jun 2020, https://reliefweb.int/disaster/fl-2020-000172-mmr.

over the polar region.[51] In June, western Siberia was influenced by both anticyclones from the west and western cyclones drooping from the north; all these factors contributed to record high air temperatures (see also 1.2.3 - Sea-surface temperature and ocean heat content). A prolonged heatwave in the north of the Siberian Federal District and the Far Eastern Federal District, Russian Federation, led to higher-than-usual forest fire intensity. The summer was very hot in parts of eastern Asia. For instance, Hong Kong, China had a record run of 13 consecutive hot nights, meaning a minimum temperature of 28 °C, from 19 June to 1 July, followed by 11 consecutive hot nights from 5 to 15 July. This also broke the record for the number of hot nights in a month. Viet Nam recorded strong heatwaves which lasted many days in June, with historical hot weather during more than 20 days in the Northern Delta and in the central provinces. In Japan, an intense subtropical anticyclone over the north-western Pacific Ocean continued to cover the country in August and contributed to record-breaking high temperatures in western and eastern Japan. The high temperature at Hamamatsu (41.1 °C) equalled Japan's national record on 17 August. In addition to those events, several heatwaves were reported in the central and western parts of Asia. In Kazakhstan, maximum daily temperature records were broken at many stations in January, February, May and November. At Bahrain International Airport, daily maximum temperatures exceeded 40 °C on 17 consecutive days (4–20 July).

Marine heatwaves are extreme events of unusually high water temperatures in the ocean.[52] They are triggered by processes taking place at the air-sea interface, by temperature redistribution in the ocean, and are sometimes affected by climate variability.[53] They are monitored using SST, though high water temperatures can reach depths of several hundred metres.[54] Over the past 35 years, marine heatwaves have doubled in frequency, becoming longer-lasting, more intense and more extensive, which is likely due to long-term anthropogenic change.[55]

Marine heatwaves have been reported at many areas in the global ocean, such as the extreme warming event in the East China Sea in 2016 that was linked to atmospheric forcing,[56] or the marine heatwave event off Japan in 2017 caused by anomalous ocean heat transport.[57] In 2020, the Laptev Sea experienced a particularly intense marine heatwave from June to December,[58] concurrent with record low sea-ice extent (see 1.2.5 - Cryosphere) and extreme atmospheric conditions (above-mentioned).

The other ocean areas of the region experienced category II (Strong)[59] marine heatwave conditions (reference period 1982–2011). Category III (Severe) values (reference period 1982–2011) were reached in the Bay of Bengal, in the Andaman Sea and off the north-eastern coast of Japan.[60]

---

51 C3S, 2020: Arctic Siberia's unusual warm spell continues, 7 July, https://climate.copernicus.eu/index.php/arctic-siberias-unusual-warm-spell-continues.

52 Oliver, E.C.J. et al., 2021: Marine heatwaves. *Annual Review of Marine Science*, 13: 313–342, https://doi.org/10.1146/annurev-marine-032720-095144.

53 Holbrook, N.J. et al., 2019: A global assessment of marine heatwaves and their drivers. *Nature Communications*, 10: 2624, https://doi.org/10.1038/s41467-019-10206-z.

54 Oliver et al., 2021: Marine heatwaves.

55 IPCC, 2019b: *IPCC Special Report on the Ocean and Cryosphere in a Changing Climate*.

56 Tan H. and R. Cai, 2018: What caused the record-breaking warming in East China Seas during August 2016? *Atmospheric Science Letters*, 19(10): e853, https://doi.org/10.1002/asl.853.

57 Sugimoto, S. et al., 2021: Local atmospheric response to the Kuroshio large meander path in summer and its remote influence on the climate of Japan. *Journal of Climate*, 34(9): 3571–3589, https://doi.org/10.1175/JCLI-D-20-0387.1.

58 WMO, 2021: *State of the Global Climate 2020*.

59 Hobday, A.J. et al., 2018: Categorizing and naming marine heatwaves. *Oceanography*, 31(2): 162–173, https://doi.org/10.5670/oceanog.2018.205.

60 WMO, 2021: *State of the Global Climate 2020*.

1.3.3 TROPICAL CYCLONES

North-west Pacific and South China Sea

In 2020, 23 Tropical Cyclones (TCs) with maximum sustained wind speeds of ≥ 34 knots formed over the western North Pacific and the South China Sea, which was below the normal of 25.6 (1981–2010 average)[61]. Tropical cyclone activities in these regions were below the climatological normal, and it is especially notable that no typhoon developed in July. From August to December, tropical cyclone activity in the region was above normal and affected countries and areas in eastern and south-eastern Asia.

In addition to one of the strongest TC of 2020, Typhoon *Goni* (*Rolly*)[62], the western North Pacific reported a number of TCs that brought devastating damage to the region. Some tropical cyclones that formed over the Philippine Sea and the South China Sea hit mainland South-East Asia. For Viet Nam, October was the month with the highest TC frequency in 2020, with four TCs directly affecting the central provinces of the country. The successive TCs, combined with the cold air inflow, caused heavy rains, big floods, flash floods and landslides in the central regions of Viet Nam, leading to loss of life and serious damages (see also 2.1 - Impact of extreme weather events in 2020). Four[63] of the 23 TCs, *Jangmi* (*Enteng*), *Bavi* (*Igme*), *Maysak* (*Julian*) and *Haishen* (*Kristine*), made landfall on the Korean Peninsula during August and September and affected north-eastern China. On 2–3 September, Typhoon *Maysak* (*Julian*) brought high winds and heavy rainfall to the Republic of Korea. During that period, accumulated precipitation of more than 1 037 mm was recorded at Seogwipo on Jeju Island. Moreover, a peak gust speed of 46 m/s was recorded in Gyeongsang Province and high waves of 8–12 m were observed in the seas to the south and east of the Korean Peninsula.

Northern Indian Ocean

In 2020, five tropical cyclones with maximum sustained wind speeds of ≥ 34 knots formed over the North Indian Ocean, and all of them made landfall. One cyclone formed over the Arabian Sea and four cyclones formed over the Bay of Bengal, resulting in near-normal cyclone activity over the Arabian Sea (1.0 tropical cyclone formed on average 1981–2010[64]) and above-normal cyclone activity over the Bay of Bengal (2.9 tropical cyclones formed on average 1981–2010). In May 2020, Cyclone *Amphan*, which was the first super cyclone over the Bay of Bengal since the Odisha super cyclone of 1999, formed during the pre-monsoon season. It crossed the West Bengal–Bangladesh coasts in the Sundarbans region as a very severe cyclonic storm on 20 May, claiming about 90 casualties (see also 2.1.1 - Affected populations and damage and 2.1.2 - Population displacement). Cyclone *Nivar*, the first cyclonic storm over the Bay of Bengal during the 2020 post-monsoon season, caused intense rainfall over the south-eastern part of India during 24–26 November.

1.3.4 OTHER EXTREME EVENTS

Sandstorms

Sand and dust storms occur when strong winds blow over exposed dry loose soil, a condition common in semi-arid and arid regions. Sandstorms occur relatively close to the ground surface, but finer dust particles can be lifted several kilometres high into the atmosphere and strong winds transport them for long distances, even across continents and oceans (Figure 16). Sand and dust storms have become an increasing concern among governments and the international community because of their damaging effects on human health, agricultural land, infrastructure and

61 RSMC Tokyo - Typhoon Center, http://www.jma.go.jp/jma/jma-eng/jma-center/rsmc-hp-pub-eg/climatology.html.

62 Names in parentheses are alternative local names for the storms attributed by the Philippine Atmospheric, Geophysical and Astronomical Services Administration.

63 Ibid.

64 Regional Specialized Meteorological Centre for Tropical Cyclone over North Indian Ocean. Frequency of formation of cyclone, https://rsmcnewdelhi.imd.gov.in/frequency-of-formation-of-cyclone.php.

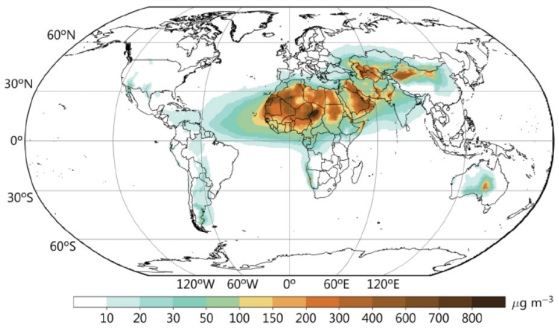

Figure 16. Annual mean surface concentration of mineral dust in 2020. *Source:* WMO Airborne Dust Bulletin, No.5 (July 2021).

transport.[65] The frequency and intensity of dust storms are increasing owing to land-use and land-cover changes and climate-related factors particularly in regions such as the Arabian Peninsula and the broader Middle East, as well as Central Asia.[66] On the other hand, a decreasing trend is seen in East Asia[67] associated with changes in wind speed and shear.[68] Many studies have shown that projects targeting desertification in China have generally played an active role in combating desertification and dust storms in China over the past several decades.[69]

Saudi Arabia experienced major sand and dust storms on 9 and 10 May. For most hours of the two days, winds exceeded 56 km/h and visibility was very poor in the country's central region (less than 1 km in Riyadh). In the spring of 2020, there were seven sand and dust storms in northern China, 10 fewer than the normal of 1981–2010. The strongest sand and dust storm occurred in north-western China during 8–10 March, which affected agricultural facilities, aircraft shipping and air pollution.

65 United Nations Environment Programme (UNEP), WMO and United Nations Convention to Combat Desertification (UNCCD), 2016: *Global Assessment of Sand and Dust Storms*. Nairobi, UNEP.

66 IPCC, 2019a: *Climate Change and Land*.

67 National Aeronautics and Space Administration (NASA), Earth Observatory, 2019: A decline in Asian dust, https://earthobservatory.nasa.gov/images/146175/a-decline-in-asian-dust.

68 Guo, J. et al., 2019: The trend reversal of dust aerosol over East Asia and the North Pacific Ocean attributed to large-scale meteorology, deposition, and soil moisture. *Journal of Geophysical Research: Atmospheres*, 124(19): 10450–10466, https://doi.org/10.1029/2019JD030654.

69 IPCC, 2019a: *Climate Change and Land*, 3.7.2.1.

PART II – RISKS AND IMPACTS

2.1 IMPACT OF EXTREME WEATHER EVENTS IN 2020

Climate-related hazards, especially floods, storms and droughts, affect people and their livelihood in many parts of Asia: High flood impacts are frequently reported in the transboundary river basins of the Indus and Ganges-Brahmaputra River in South Asia. Tropical cyclones/typhoons hit countries in South-East Asia, East Asia and South Asia. Droughts often result in high socioeconomic and environmental impacts in several parts of the region. Moreover, the COVID-19 pandemic complicated disaster management efforts and countries faced the dual challenge of tackling the pandemic and climate-related hazards. This was particularly the case during high-impact events, such as floods and storms (Figure 17).

2.1.1 AFFECTED POPULATIONS AND DAMAGE

In 2020, floods and storms affected approximately 50 million people including over 5 000 lives lost.[70] This is below the annual average of the last two decades: 158 million people affected and about 15 500 fatalities.[71] As regards damage, India and China suffered the most in absolute value from extreme

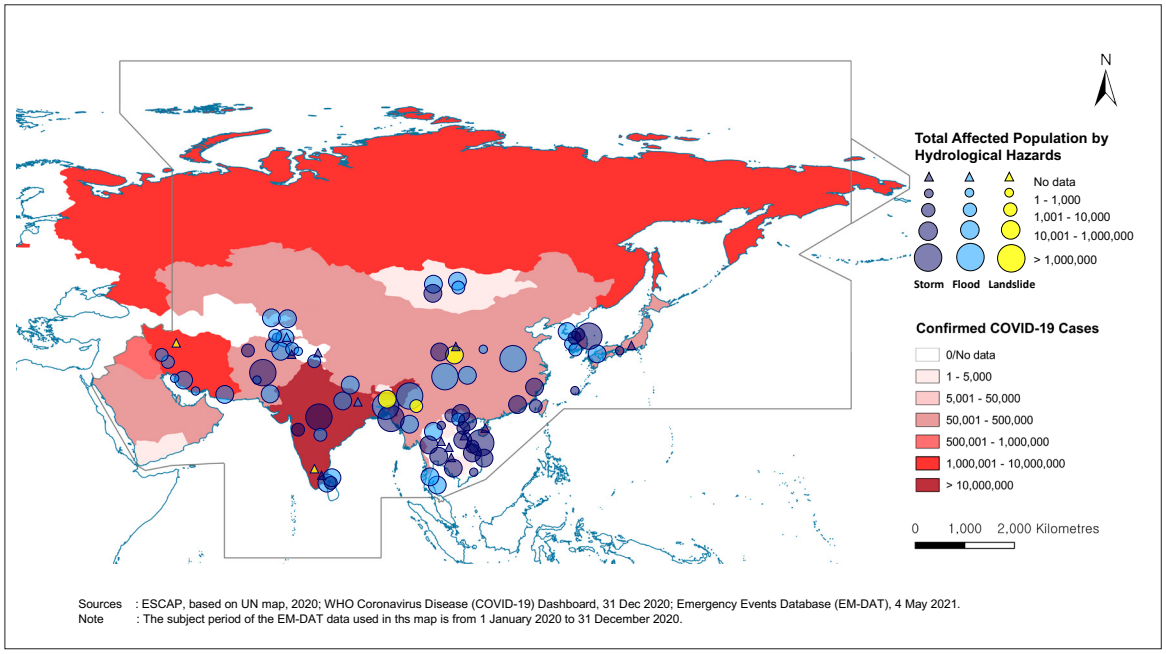

Figure 17. Climate-related hazards converging with COVID-19 in 2020. *Sources*: Economic and Social Commission for Asia and the Pacific (ESCAP); World Health Organization (WHO); Centre for Research on the Epidemiology of Disasters (CRED), International Disaster Database (EM-DAT). Note: The period of the EM-DAT data used in this map is from 1 January to 31 December 2020. *Source:* ESCAP, based on UN map, 2020; WHO Coronavirus Disease (COVID-19) Dashboard, 31 Dec 2020; Emergency Events Database (EM-DAT), 4 May 2021.

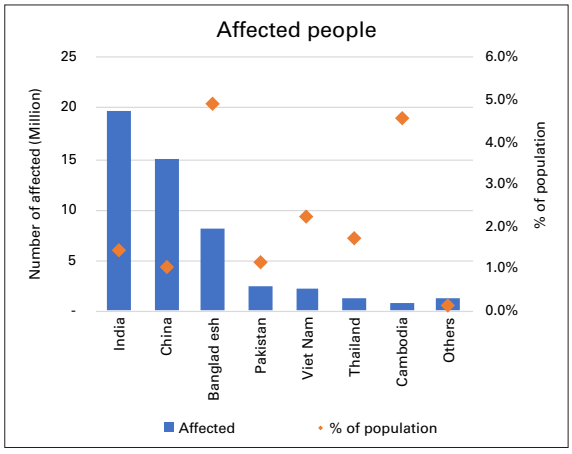

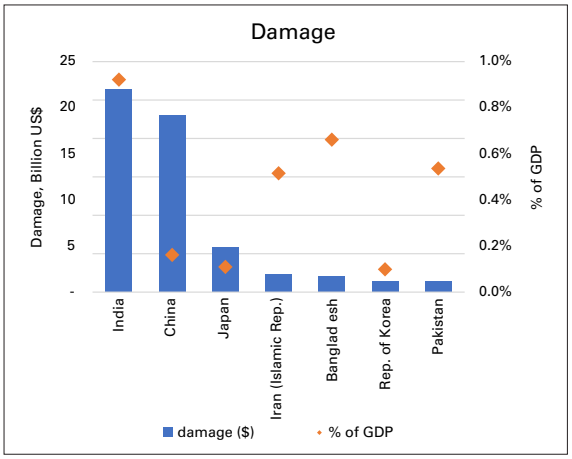

Figure 18. Affected people and damage by climate-related hazards in Asia in 2020. *Source:* CRED EM-DAT (data on people affected and damage by climate-related hazards); ESCAP Sustainable Development Goals Gateway Data (https://dataexplorer.unescap.org) (data on population and GDP)

70 CRED EM-DAT, www.emdat.be

71 Ibid.

events: US$ 26.3 billion and US$ 23.1 billion, respectively. Japan, the Islamic Republic of Iran, Bangladesh and the Republic of Korea also suffered severe damage. For some countries the impact was significant when translated into percentage of gross domestic product (GDP), which was the case for India, the Islamic Republic of Iran, Bangladesh and Pakistan, where damages exceed 0.5% of GDP. Figure 18 shows the number of affected people and damage associated with extreme events in the region, in absolute numbers (blue bars) and percentage (orange markers) with reference to total population and GDP.

Cyclone *Amphan*, one of the strongest cyclones ever recorded, hit densely populated coastal areas in Bangladesh and India during the rapid spread of COVID-19 in May 2020[72] (see also 1.3.3 - Tropical cyclones). It is an exemplary case where the affected countries faced the dual challenge of tackling a pandemic and the impact of an extreme event. The response to the impact of *Amphan* was made difficult owing to restrictions imposed during the pandemic and the disruption of supply chains.[73]

Impacts of other high-impact events in specific locations include:

- *Afghanistan (floods)* – In August, floods caused heavy rainfall to hit 14 provinces.[74] Approximately 2 400 houses were damaged and over 1 550 houses were destroyed.[75]
- *Bangladesh and India* (*Cyclone* Amphan) – In May, Cyclone *Amphan* made landfall in India and Bangladesh. In India, in West Bengal, 86 lost their lives and 13.6 million people were affected.[76] Damage amounted to approximately US$ 14 billion.[77] Bangladesh reported total damage of more than US$ 130 million. A total of 10 million people in 19 districts were affected, and more than 330 000 houses were damaged[78] (see also 1.3.3 - Tropical cyclones).
- *China* (*floods and Typhoon* Hagupit) – A heavy rainfall event in June–July in the middle and lower reaches of the Yangtze River affected 27 provinces and 63 million people. It also led to a direct loss of US$ 26 billion[79] (see also 1.3.1 - Extreme rainfall and floods). Typhoon *Hagupit* hit China in August. Approximately 12 000 fishing vessels were called back to harbour, and transportation, power supply, aquaculture, fishery and tourism were interrupted.[80]
- *Japan* (*floods and Typhoon* Haishen) – A persistent heavy rainfall event in July caused flooding. A total of 961 sediment-related disaster events (e.g. landslides) associated with the rainfall were reported across 37 prefectures, one of the highest numbers from extreme weather events in Japan. Particularly in Kumamoto Prefecture, 227 such disaster events occurred, the highest number on record for a prefecture

72 ESCAP, 2020: Protecting the Most Vulnerable to Cascading Risks from Climate Extremes and the COVID-19 in South Asia, https://www.unescap.org/resources/protecting-most-vulnerable-cascading-risks-climate-extremes-and-covid-19-south-asia.

73 CARE Bangladesh, United Nations Office for Project Services (UNOPS) and UK aid, 2020: Cyclone Amphan joint needs assessment, 31 May, https://reliefweb.int/sites/reliefweb.int/files/resources/cyclone_amphan_joint_needs_assessment_final_draft_31052020.pdf.

74 The affected provinces were Parwan, Maidan Wardak, Kabul, Kapisa, Logar, Nuristan, Kunar, Laghman, Nangarhar, Panjshir, Khost, Paktia, Paktika and Ghazni.

75 International Federation of Red Cross and Red Crescent Societies (IFRC), 2021: *Final Report. Afghanistan: Flash floods*, 31 May, https://reliefweb.int/sites/reliefweb.int/files/resources/MDRAF006dfr.pdf.

76 State Inter Agency Group - West Bengal, 2020: *Joint Rapid Need Assessment Report on Cyclone Amphan*, https://nidm.gov.in/covid19/PDF/covid19/state/West%20Bengal/223.pdf.

77 WMO, 2021: *State of the Global Climate 2020*.

78 CARE Bangladesh, UNOPS and UK aid, 2020: Cyclone Amphan joint needs assessment.

79 Hayes, D. et al., 2020: The impact of flooding on China's agricultural production and food security in 2020. *Agricultural Policy Review*. Center for Agricultural and Rural Development, Iowa State University, www.card.iastate.edu/ag_policy_review/article/?a=115.

80 China member report presented to the 15th Integrated Workshop of the ESCAP/WMO Typhoon Committee, December 2020, http://www.typhooncommittee.org/15IWS/Members15IWS.html.

from an extreme event[81] (see also 1.3.1 - Extreme rainfall and floods). In September, Typhoon *Haishen* brought heavy rainfall in Miyazaki Prefecture. It resulted in two fatalities, four people missing and 111 injured. It damaged electricity and water supply infrastructure, causing power outages for 69 720 residences.[82]

- *Mongolia (flash floods)* – In July and August, flash floods and heavy rainfall affected over 3 570 households and essential infrastructure, including main roads, bridges and electricity sub-stations in 11 provinces and three districts. About 14 000 m^2 of public area, 7 300 m^2 of sidewalk and 13 100 m of bitumen roads were damaged.[83]

- *Pakistan (floods)* – During August and early September, Pakistan was severely hit by monsoon rains, resulting in 409 fatalities, 402 injured and 305 151 fully or partially damaged homes[84] (see also 1.3.1 - Extreme rainfall and floods).

- *Viet Nam* (*Typhoon Molave and Tropical Storm* Linfa) – In October, Typhoon Molave hit Viet Nam and caused 40 fatalities and 140 injured.[85] More than 310 000 homes were damaged,[86] as well as 28 000 hectares of rice and crops.[87] Vital infrastructure, such as electricity and roads, was also damaged, causing disruption in service delivery and assistance.[88] In addition, Tropical Storm *Linfa* resulted in 138 fatalities and 16 missing; 16 692 hectares of rice and crops were flooded; and 105 090 tons of food got wet or washed away (see also 1.3.3 - Tropical cyclones).[89]

2.1.2 POPULATION DISPLACEMENT

Climate and weather events had major and diverse impacts on population movements and on the vulnerability of people on the move in Asia throughout 2020. Much of the disaster-related displacement recorded globally in 2020 took place in China, Bangladesh and India, which recorded some of the highest figures (about 4 to 5 million new displacements each).[90] Refugees, internally displaced people and migrants in Asia are often among those most vulnerable to climate-related and weather-related hazards.[91] The overwhelming majority of weather-related displacements in Asia take place within national borders, though cross-border movements also occur.

Additionally, mobility restrictions and economic downturns due to COVID-19 have slowed the delivery of humanitarian assistance to vulnerable people on the move, as well as efforts to support recovery for

81 Ministry of Land, Infrastructure, Transport and Tourism, Japan, 2020, https://www.mlit.go.jp/report/press/sabo02_hh_000112.html.

82 Japan member report presented to the 15th Integrated Workshop of the ESCAP/WMO Typhoon Committee, December 2020, http://www.typhooncommittee.org/15IWS/Members15IWS.html.

83 IFRC, 2021: *Final Report. Mongolia: Flash floods*, 1 February, https://reliefweb.int/sites/reliefweb.int/files/resources/MDRMN012dfr.pdf.

84 European Commission's Directorate-General for European Civil Protection and Humanitarian Aid Operations (DG ECHO), 2020: Pakistan - Monsoon rains and floods (ECHO Daily Flash of 29 October 2020), https://reliefweb.int/report/pakistan/pakistan-monsoon-rains-and-floods-dg-echo-echo-daily-flash-29-october-2020.

85 Association of South-East Asian Nations (ASEAN) Food Security Information System, 2020: Typhoon Molave effects toward food security in Vietnam, 24 November, http://www.aptfsis.org/news-events/news44.

86 IFRC, 2020: Homes of 1 million people in ruin as major typhoon hits Viet Nam. Press release, 28 October, https://media.ifrc.org/ifrc/press-release/homes-1-million-people-ruin-major-typhoon-hits-viet-nam/.

87 ASEAN Food Security Information System, 2020: Typhoon Molave effects toward food security in Vietnam.

88 United Nations News, 2020: Millions affected as devastating typhoon strikes Viet Nam. Press release, 29 October, https://news.un.org/en/story/2020/10/1076412.

89 Viet Nam member report presented to the 15th Integrated Workshop of the ESCAP/WMO Typhoon Committee, November 2020, http://www.typhooncommittee.org/15IWS/Members15IWS.html.

90 Internal Displacement Monitoring Centre, 2021: *Global Report on Internal Displacement 2021*, https://www.internal-displacement.org/global-report/grid2021/.

91 Office of the United Nations High Commissioner for Refugees (UNHCR). Climate change and disaster displacement, https://www.unhcr.org/climate-change-and-disasters.html.

affected persons, including durable solutions for those displaced.[92] The vulnerabilities of displaced populations, often living in densely populated settlements in Asia, were further amplified.[93] Many displacement situations triggered by hydrometeorological events in Asia have become prolonged or protracted for people unable to return to their former homes or without options for integrating locally or settling elsewhere.

In May, Cyclone *Amphan* (see also 1.3.3 - Tropical cyclones) hit the Sundarbans region between India and Bangladesh, displacing 2.4 million people in India, mostly in West Bengal and Odisha, and 2.5 million people in Bangladesh. While many returned relatively soon afterwards, damage to more than 2.8 million homes likely resulted in homelessness and prolonged displacement for many thousands. Many displaced people did not have access to evacuation centres and were compelled to take shelter in tents or in the open air on embankments.[94]

Intense cyclones, monsoon rains and floods hit highly exposed and densely populated areas in South Asia and East Asia and led to the displacement of millions of people in China, Bangladesh, India, Japan, Pakistan, Nepal and Viet Nam (see also 1.3.1 - Extreme rainfall and floods). China and Bangladesh each recorded more than 4 million new displacements, many of them pre-emptive evacuations.[95] During monsoon seasons, torrential rainfall sweeps through the Rohingya refugee settlements in Cox's Bazar, Bangladesh, causing flooding and landslides that force the refugees living there to be displaced once again.[96]

In July 2020, flooding and landslides affected several districts across Nepal. The International Organization for Migration (IOM) assessments in August showed the presence of a total of 5 467 persons from 1 066 households residing in 29 displacement sites across the country.[97] By September 2020, only 12 sites were still active, hosting some 2 000 individuals in three districts, as people returned home with the end of the monsoon season.[98]

In October, Cyclone *Molave*, the fourth storm of the month to hit Viet Nam, triggered the evacuation of some 1.3 million people (see also 1.3.3 - Tropical cyclones).[99]

2.1.3 AGRICULTURE AND FOOD SECURITY

In Asia, progress on food security and nutrition has slowed down and is not on track to achieve the Sustainable Development Goal targets of ending hunger and all forms of malnutrition by 2030 (targets 2.1 and 2.2). In 2020, 48.8 million people in South-East Asia, 305.7 million in South Asia and 42.3 million in West Asia are estimated to have been undernourished. Asia accounts for more than half of the global total. Most children under 5 years of age with stunting or wasting in the region are found in South Asia (54.3 million and 25.0 million, respectively, in 2020). The true impacts of COVID-19 on food security and nutrition are yet to be established but compared with 2019, the number of undernourished people in 2020 increased by 6% in South-East Asia and West Asia, and by 20% in South Asia. Larger increases in

92 Gaynor, T., 2020: Climate change is the defining crisis of our time and it particularly impacts the displaced. UNHCR, 30 November, https://www.unhcr.org/news/latest/2020/11/5fbf73384/climate-change-defining-crisis-time-particularly-impacts-displaced.html.

93 UNHCR and Potsdam Institute for Climate Impact Research, 2020: COVID-19, displacement and climate change, June, https://www.unhcr.org/protection/environment/5ef1ea167/covid-19-displacement-climate-change.html.

94 Siegfried, K., 2020: The refugee brief – 22 May 2020, UNHCR, https://www.unhcr.org/refugeebrief/the-refugee-brief-22-may-2020/.

95 Internal Displacement Monitoring Centre, 2021: *Global Report on Internal Displacement 2021*.

96 UNHCR. Displaced on the frontlines of the climate emergency, https://storymaps.arcgis.com/stories/065d18218b654c798ae9f360a626d903

97 IOM, 2020: Displacement Tracking Matrix: Nepal – landslide and floods site assessment, 7 September, https://dtm.iom.int/reports/nepal-%E2%80%93-landslides-and-floods-displacement-%E2%80%93-site-assessment-report-september-2020.

98 IOM, 2020: Displacement Tracking Matrix: Nepal – landslide and floods site assessment (round 2), 14 October, https://dtm.iom.int/reports/nepal-%E2%80%93-landslides-and-floods-displacement-%E2%80%93-site-assessment-round-2-october-2020.

99 WMO, 2021: *State of the Global Climate 2020*.

undernourishment were seen in countries that were also affected by other drivers, particularly climate-related disasters.[100]

The efforts of international organizations, in particular FAO and WFP, to alleviate the acute food security situation were welcomed by the beneficiary communities. A review conducted by OCHA shows a general satisfaction among the beneficiaries of the aid which helped in improving the life conditions of those communities.

The assessed major impacts on agriculture and food security are summarized below:

In Japan, floods in July heavily affected the agriculture sector, with the loss and damage totalling over US$ 2 billion. In addition, 13 146 hectares of cropland were affected, with an estimated loss and damage of US$ 935 million across 40 prefectures. Forestry also suffered greatly with loss and damage of US$ 879 million[101] (see also 1.3.1 - Extreme rainfall and floods).

In Afghanistan, floods in August also heavily affected agriculture, which washed away crops and weakened agricultural irrigation systems, agricultural lands and livestock in regions where the vast majority of the affected population rely economically on agriculturally based livelihoods.[102]

In China, floods during the summer monsoon period led to increased prices for domestic meat and vegetables in the affected provinces, but not for grain prices owing to increased grain imports.[103] Moreover, a heavy rainfall event in June–July and floods in the middle and lower reaches of the Yangtze River affected 27 provinces and 6.03 million hectares of cropland (23%), with 1.14 million hectares of crop failure (4%). The total summer crop sown area in 2020 was 26.17 million hectares in the basin.[104]

In Yemen, food security and nutrition has deteriorated significantly owing to a confluence of conflict, displacement, economic collapse, COVID-19, and flooding during April–August. Although the disaggregated impact of climate extremes is difficult to quantify among the other drivers, climate extremes contributed to a worsening of the food insecurity situation. Yemen has been a reservoir and source area for desert locusts due to continual and widespread rains since 2018, in the interior and coastal areas. Since late 2019, the worst upsurge in desert locusts in 25 years in eastern Africa and Yemen has happened, supported by widespread heavy rainfall in the area. In the Arabian Peninsula, surveillance and control operations had to be conducted and over 220 000 hectares were treated, including in Yemen (50 000 hectares).[105] Nevertheless, there was growing evidence that the upsurge was receding thanks to joint surveillance and control operations and less favourable climate conditions for desert locusts since late 2020.[106]

In Bangladesh, Cyclone *Amphan* damaged more than 176 000 hectares of agricultural land (crops and fish/shrimp farms) and 14 000 livestock were lost[107] (see also 1.3.3 - Tropical cyclones). The floods in June led

---

100 Food and Agriculture Organization of the United Nations (FAO), International Fund for Agricultural Development (IFAD), United Nations Children's Fund (UNICEF), World Food Programme (WFP) and WHO, 2021: *The State of Food Security and Nutrition in the World 2021. Transforming Food Systems for Food Security, Improved Nutrition and Affordable Healthy Diets for All*. Rome, FAO, https://doi.org/10.4060/cb4474en.

101 Ministry of Agriculture, Forestry and Fisheries, Japan, 2021, https://www.maff.go.jp/j/saigai/ooame/r0207.

102 IFRC, 2021: Final Report. *Afghanistan: Flash floods*.

103 Hayes et al., 2020: The impact of flooding on China's agricultural production and food security in 2020.

104 Ibid.

105 FAO, 2020: *Greater Horn of Africa and Yemen – Desert Locust Crisis Appeal (January 2020–June 2021): Revised Appeal for Sustaining Control Efforts and Protecting Livelihoods (Six-Month Extension)*. Rome, FAO, http://www.fao.org/emergencies/resources/documents/resources-detail/en/c/1364948/.

106 FAO, 2021: *Desert Locust Upsurge – Progress Report on the Response in the Greater Horn of Africa and Yemen (January–April 2021)*. Rome, FAO, http://www.fao.org/emergencies/resources/documents/resources-detail/en/c/1410821/.

107 CARE Bangladesh, UNOPS and UK aid, 2020: Cyclone Amphan joint needs assessment.

to the loss of US$ 74.5 million worth of livestock.[108] They also disrupted the functioning of local markets, and the majority of unions reported irregular food consumption and complication in food preparation, such as limited availability of or access to firewood and safe water. Using a 10-day forecast, FAO managed to support over 18 000 households ahead of flood peaks, delivering livestock feed and storage drums to 83% of households.[109] It was also the first ever coordinated multi-agency anticipatory approach for a sudden-onset hazard and was executed in collaboration with OCHA, the Bangladesh Red Crescent Society, WFP and the United Nations Population Fund. The agencies acted in tandem on the same early warning trigger and implemented activities simultaneously in a coordinated way before the floods peaked. Thanks to the pre-agreed framework, the Central Emergency Response Fund released US$ 2.8 million ahead of a flood warning to United Nations agencies and partners in only four hours – the fastest allocation of United Nations resources in history.[110]

2.2 UNDERSTANDING CLIMATE IMPACTS FOR BETTER CLIMATE ADAPTATION POLICIES

Developing and improving climate-resilient economies and societies require a good understanding of climate-related risks and climate impacts on a long-term basis. Extreme events are amplified by climate change; at the same time, population growth, urbanization and the development of economic assets enhance exposure to climate risks. The end result is increased costs on various development indicators, which can be aggregated in terms of impact on economic growth and influence on achieving the Sustainable Development Goals.

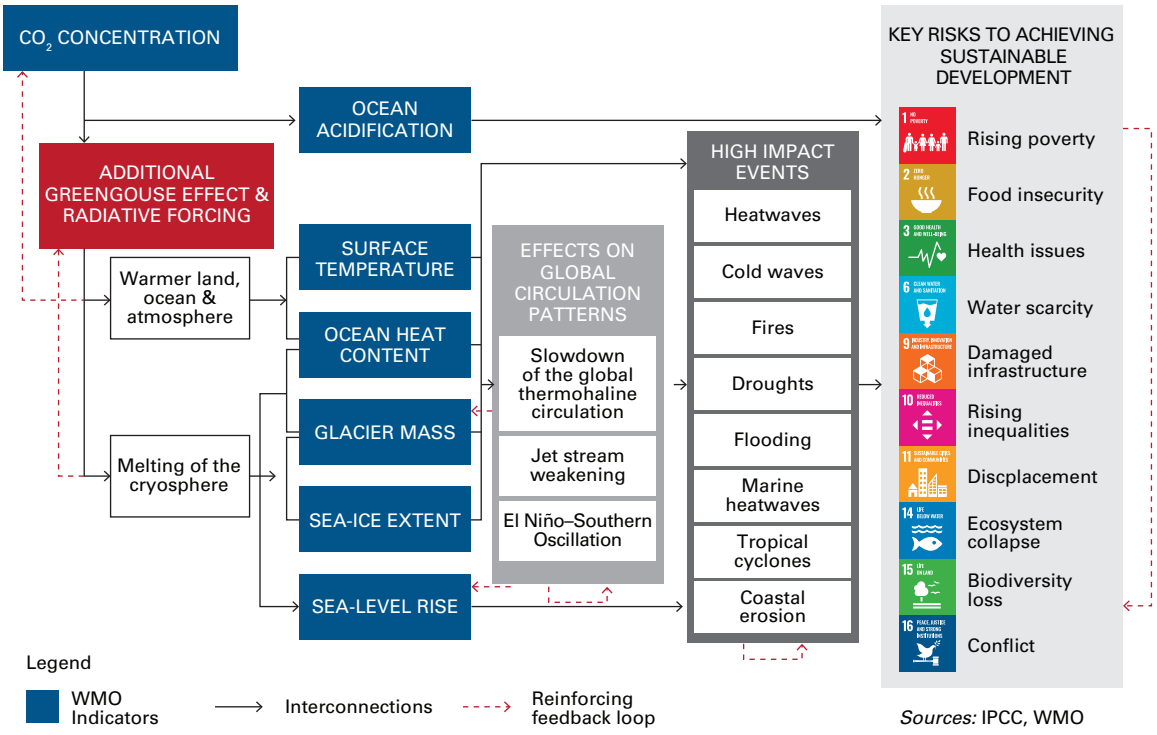

Figure 19. Selected climate change-related risks to the achievement of the Sustainable Development Goals. *Source:* WMO, 2021: *Climate Indicators and Sustainable Development: Demonstrating the Interconnections* (WMO-No. 1271).

Sources: IPCC, WMO

108 IFRC, 2021: *Final Report. Bangladesh: Monsoon Floods*, 5 May, https://reliefweb.int/sites/reliefweb.int/files/resources/MDRBD025efr%20%281%29.pdf.

109 FAO, 2021: *Bangladesh – Impact of Anticipatory Action. Striking Before the Floods to Protect Agricultural Livelihoods.* Dhaka, FAO, http://www.fao.org/3/cb4113en/cb4113en.pdf.

110 Central Emergency Response Fund, 2020: *Bangladesh Rapid Response Anticipatory Action Pilot Flood*, https://cerf.un.org/sites/default/files/resources/20-RR-BGD-44022_Bangladesh_CERF_Report.pdf.

The United Nations sustainable development agenda provides a universally agreed framework for achieving the Sustainable Development Goals. However, the achievement of the Goals can be hampered by the impact of climate change (Figure 19).[111]

This section discusses the relationship between the impacts of extreme events and sustainable development, to inform. adaptation policies in the light of the evolving climate-related risks knowledge in the region and the lessons learned from climate impacts recorded in 2020.

2.2.1 COST OF EXTREME WEATHER EVENTS AND SUSTAINABLE DEVELOPMENT

Extreme weather events continue to threaten sustainable development: Tropical cyclones, floods and droughts induced an estimated average annual loss (AAL) of several hundred billion dollars. China, India and Japan experienced the majority of this loss: approximately US$ 238 billion in China, US$ 87 billion in India and US$ 83 billion in Japan (Figure 20). When the size of the economy is considered, AAL is expected to be as high as 7.9% of GDP (US$ 7.5 billion) for Tajikistan, 5.9% of GDP (US$ 24.5 billion) for Cambodia and 5.8% of GDP (US$ 17.9 billion) for the Lao People's Democratic Republic. The highest AALs are associated with drought.[112]

Increased negative impacts on inequality and poverty: In the Asia-Pacific Disaster Report 2017, it was mentioned that globally the occurrence of a natural disaster increases the Gini index, a common measure of inequality, by 0.01 in the next year, and it was estimated that for this region the increase is higher.[113] Moreover, disasters affect mainly the poor, as wealthier people can afford to protect their assets and well-being from natural disasters and avoid living in disaster-prone areas.[114]

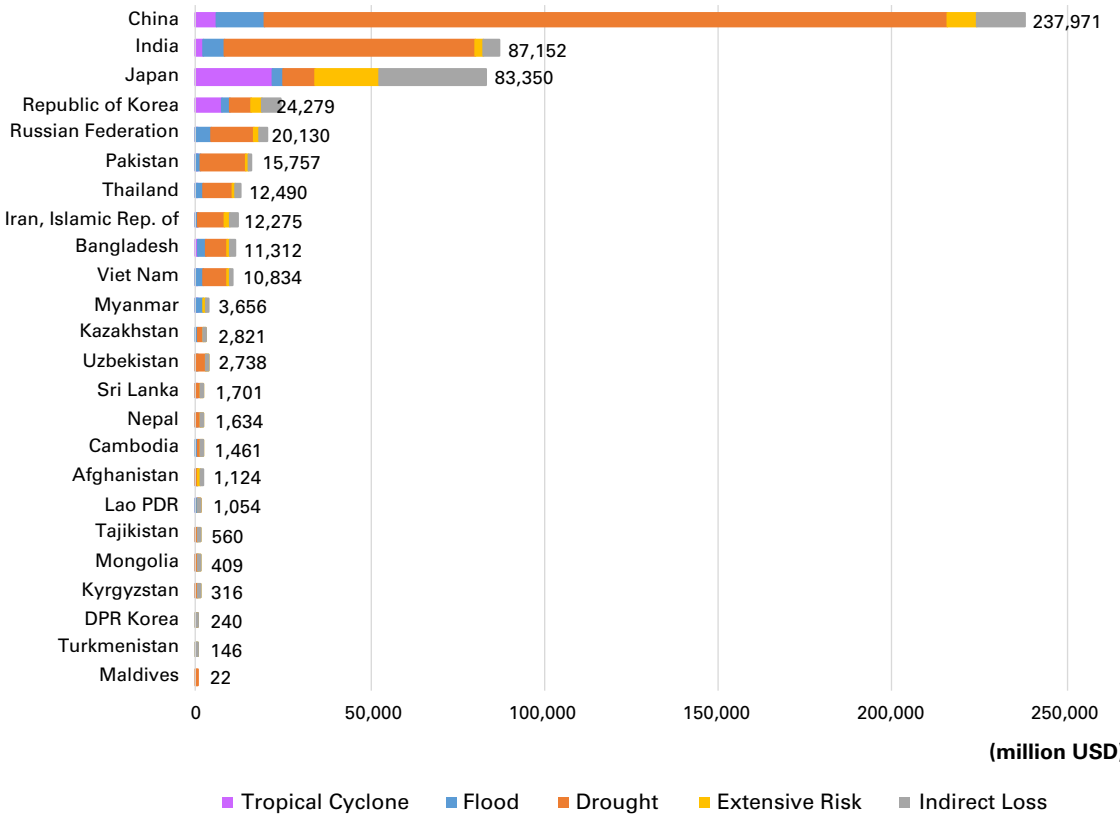

Figure 20. Total AAL from climate-related hazards in Asia. Data sourced from ESCAP, 2021: The Risk and Resilience Portal. Note: Data unavailable for Bahrain; Bhutan; Hong Kong, China; Iraq; Kuwait; Macao, China; Oman; Qatar; Saudi Arabia; United Arab Emirates; and Yemen.

111 WMO, 2021: *Climate Indicators and Sustainable Development: Demonstrating the Interconnections* (WMO-No. 1271). Geneva.

112 ESCAP, 2021: The Risk and Resilience Portal. https://rrp.unescap.org/economic-impacts/economic-impact

113 ESCAP, 2017: *Asia-Pacific Disaster Report 2017: Disaster Resilience for Sustainable Development*. Bangkok, United Nations, https://www.unescap.org/publications/asia-pacific-disaster-report-2017-leave-no-one-behind.

114 ESCAP, 2019: *Asia-Pacific Disaster Report 2019: The Disaster Riskscape Across Asia-Pacific – Pathways for Resilience, Inclusion and Empowerment*. Bangkok, United Nations, https://www.unescap.org/publications/asia-pacific-disaster-report-2019.

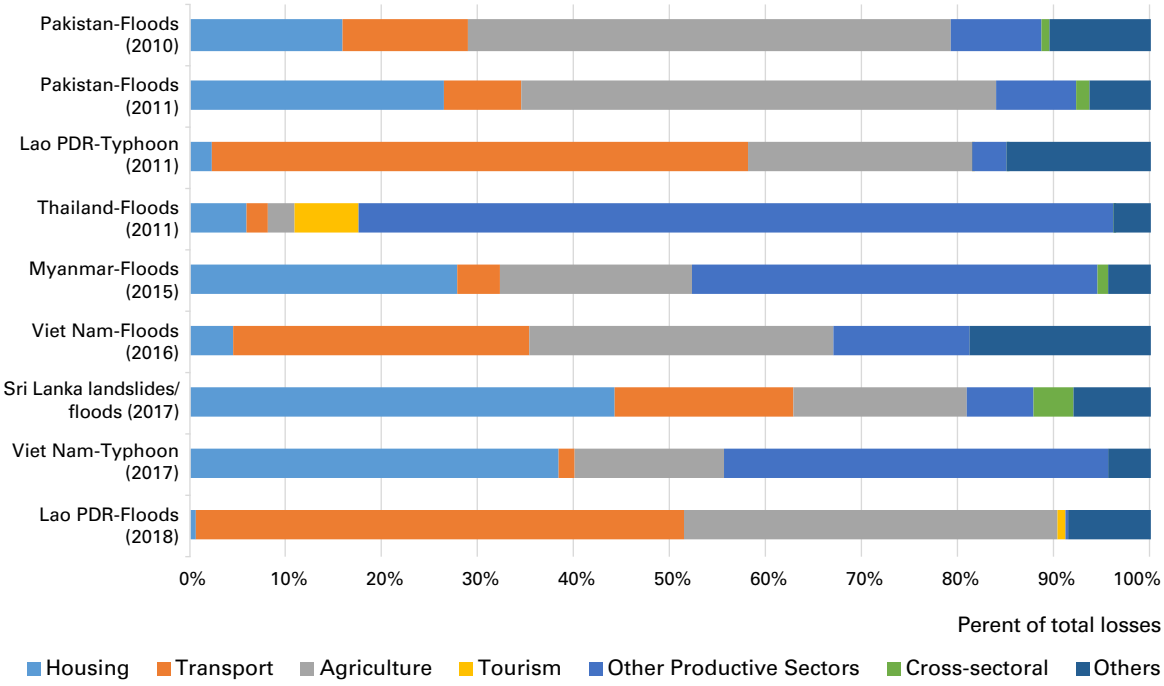

Figure 21. Examples of damage and losses by sector from major disasters. *Sources*: Post-Disaster Needs Assessment reports collected from the Global Facility for Disaster Reduction and Recovery; World Bank; State Inter Agency Group - West Bengal, 2020: *Joint Rapid Need Assessment Report on Cyclone Amphan*

Disruptive effects on socioeconomic indicators: Post-disaster needs assessments for extreme weather events demonstrate the events' impacts on various economic sectors, from housing, transport and agriculture to other productive sectors (Figure 21). For instance, the damage associated with Cyclone *Amphan* was mostly to social infrastructure (e.g. housing, schools and hospitals), physical infrastructure (e.g. energy, transport, water/sanitation and communication networks) and agriculture (e.g. crops and livestock).[115] The costs of extreme events are rising because a high proportion of existing critical infrastructures are in multi-hazard risk hotspots, which can lead to significant disruption in economic activity when natural disasters occur. For instance, about a third of energy power plants, fibre-optic cable networks and airports, and 42% of road infrastructure, are in multi-hazard risk hotspots.[116]

Although damage and losses in sectors differed from event to event based on the varying characteristics of the affected region, they all led to large impacts on the sectors with implications on key socioeconomic indicators, such as transportation cost, employment, food security and trade.

Economy and infrastructure at high risk: In Viet Nam, impacts from weather and climate disasters, like Typhoon Damrey in November 2017, can lead to a significant reduction of GDP, e.g. about one percent point of annual growth, with the agriculture sector being the worst affected.[117] Climate change would reduce national income by up to an estimated 3.5% by 2050.[118] In Japan, massive storm surges and large-scale river floods are expected to have devastating impacts on key manufacturing hubs in Tokyo, Osaka and Nagoya.[119]

115 ESCAP, 2020: Time and tide wait for no man, 23 June, https://www.unescap.org/blog/time-and-tide-wait-no-man.

116 ESCAP, 2019: *Asia-Pacific Disaster Report 2019*.

117 World Bank, 2018: *2017 Vietnam Post-Typhoon Damrey Rapid Damage and Needs Assessment. Khanh Hoa Provincial Peoples' Committee*. Washington, DC, World Bank, https://www.gfdrr.org/sites/default/files/publication/vietnam-damrey-rapid-assessment-report-en.pdf.

118 World Bank Group and Asian Development Bank (ADB), 2020: *Climate Risk Country Profile: Vietnam*, https://www.adb.org/sites/default/files/publication/653596/climate-risk-country-profile-viet-nam.pdf.

119 World Bank, 2020: *Resilient Industries in Japan: Lessons Learned in Japan on Enhancing Competitive Industries in the Face of Disasters Caused by Natural Hazards*. World Bank, Washington, DC, https://openknowledge.worldbank.org/handle/10986/34765.

Moreover, it is reported that increased heat and humidity can lead to an effective loss of outdoor working hours, putting between US$ 2.8 trillion and US$ 4.7 trillion of GDP in Asia annually at risk by 2050, on average.[120] Thus, it is important to invest in climate adaptation; the report of the Global Commission on Adaptation highlights that spending on climate adaptation is a high-return investment with multiple economic benefits.[121]

2.2.2 COMPOUNDED VULNERABILITIES FOR MIGRANTS, REFUGEES AND FORCIBLY DISPLACED PEOPLE

In Asia, many vulnerable people on the move, regardless of their reasons for moving, end up settling in high-risk areas, where they are exposed to climate and weather hazards across a range of scales. The compounding risks of displacement resulting from hydrometeorological hazards, and exacerbated by climate change, may also intersect with (or precipitate) other disasters and vulnerabilities. Consequently, it is important that disaster risk reduction measures are informed not only by specific and local disaster risks, but also by possible broader compounding risks.

For instance, specific conditions of risk from hydrometeorological disasters are particularly well documented in the Rohingya refugee sites in Cox's Bazar, Bangladesh. Over the year, a total of 162 275 people were affected, with many requiring assistance.[122,123] Without preparedness measures undertaken in the camp areas, including kits for strengthening shelters, building of retaining structures on hillsides and improving drainage, roads and bridges, these impacts would have been worse.[124]

2.2.3 ENVIRONMENTAL ISSUES AND LOSS OF NATURAL ECOSYSTEMS

While healthy ecosystems are foundational to sustainable development, climate change and related extreme events have direct negative environmental effects. These include, but are not limited to, pollutants and hazardous chemicals from flooded industrial sites entering groundwater, rivers and oceans; and wildfires, floods and storms defoliating forests and disrupting ecosystems.[125]

Climate change accelerates loss of natural assets. The characteristics of ocean and cryosphere change include thresholds of long-term changes being unavoidably exceeded and irreversibility, posing risks and challenges to adaptation.[126] One in four species is facing extinction, about one fourth of all ice-free land is subjected to degradation, and coral reefs are projected to decline by up to 99% at 2 °C of warming.[127] It is also predicted that climate change can reduce the ability of reef systems to provide food by 50% by 2050.[128]

Glaciers in the Himalayan region that have been important sources of fresh water have been receding.[129] It is projected that glacier mass will decrease by 20% to 40% by 2050,[130]

---

120 McKinsey Global Institute, 2020: *Climate Risk and Response in Asia*, https://www.mckinsey.com/business-functions/sustainability/our-insights/climate-risk-and-response-in-asia.

121 Global Commission on Adaptation, 2019: *Adapt Now: A Global Call for Leadership on Climate Resilience*, https://gca.org/wp-content/uploads/2019/09/GlobalCommission_Report_FINAL.pdf.

122 WMO, 2021: *State of the Global Climate 2020*.

123 IOM, 2020: Bangladesh: Needs and Population Monitoring portal, 12 May, https://www.arcgis.com/apps/MapSeries/index.html?appid=1eec7ad29df742938b6470d77c26575a.

124 Siegfried, K., 2020: The refugee brief – 22 May 2020, UNHCR.

125 ESCAP, 2021: *Economic and Social Survey of Asia and the Pacific 2021: Towards Post-COVID-19 Resilient Economies*. Bangkok, United Nations, https://www.unescap.org/kp/2021/economic-and-social-survey-asia-and-pacific-2021-towards-post-covid-19-resilient-economies.

126 IPCC, 2019b: *IPCC Special Report on the Ocean and Cryosphere in a Changing Climate*.

127 Global Commission on Adaptation, 2019: *Adapt Now*.

128 World Wide Fund for Nature and ADB, 2012: *Ecological Footprint and Investment in Natural Capital in Asia and the Pacific*. Manila and Geneva, https://www.adb.org/publications/ecological-footprint-and-investment-natural-capital-asia-and-pacific.

129 Global Center on Adaptation, 2020: *State and Trends in Adaptation Report 2020*, https://gca.org/reports/state-and-trends-in-adaptation-report-2020/.

130 Considering the RCP 8.5 high-emission pathway.

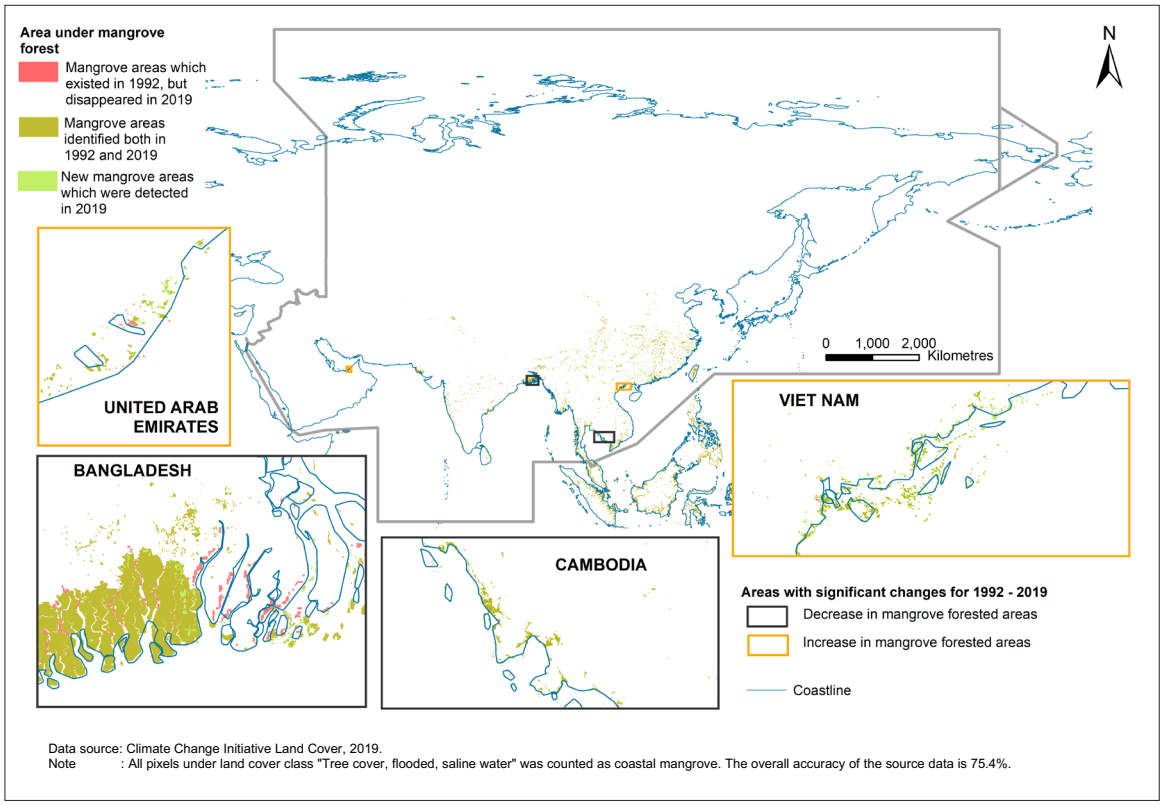

Figure 22. Changes in mangrove cover in Asia between 1992 and 2019. Data sourced from European Space Agency, Climate Change Initiative Land Cover, 2019 (http://www.esa-landcover-cci.org/?q=node/164). Note: All pixels under land cover class "Tree cover, flooded, saline water" counted as coastal mangrove. The overall accuracy of the source data is 75.4%. *Source:* Climate Change Initiative Land Cover, 2019.

affecting the lives and livelihoods of about 750 million people in the region.[131,132,133] In Afghanistan, glacial meltwater has historically been essential for maintaining water supply in times of drought, but the projected reduction in glacial run-off will exacerbate the impacts of drought on water supply in the country.[134]

Mangroves, a crucial natural ecosystem, provide coastal protection in tropical regions. While significant mangrove losses are projected due to human activities, climate change can also negatively affect mangroves through rise in sea level, in atmospheric CO2 and in air and water temperatures, as well as through change in the frequency and intensity of precipitation and storm patterns.[135] In 2019, approximately three fourths of mangroves in Asia were located in Bangladesh (24%), Myanmar (19%), India (17%) and Thailand (14%), while mangroves in Bangladesh decreased by 19% from 1992 to 2019 (Figure 22).[136]

Deforestation can also be intensified by climate change, although it is mainly attributed to human activity.[137] Between 1990 and

131 McKinsey Global Institute (MGI), 2020: Climate risk and response in Asia Future of Asia, https://www.mckinsey.com/~/media/mckinsey/business%20functions/sustainability/our%20insights/climate%20risk%20and%20response%20physical%20hazards%20and%20socioeconomic%20impacts/mgi-climate-risk-and-response-full-report-vf.pdf

132 This includes Afghanistan, Bangladesh, Bhutan, China, India, Myanmar, Nepal and Pakistan.

133 Maurer J.M. et al., 2019: Acceleration of ice loss across the Himalayas over the past 40 years. *Science Advances*, 5(6): eaav7266, https://advances.sciencemag.org/content/5/6/eaav7266.

134 World Bank Group and ADB, 2021: *Climate Risk Country Profile: Afghanistan*, https://climateknowledgeportal.worldbank.org/sites/default/files/2021-05/15396A-WB_Afghanistan%20Country%20Profile-WEB.pdf.

135 World Bank Group, 2016: *Mangroves as Protection from Storm Surges in a Changing Climate*, https://documents1.worldbank.org/curated/en/703121468000269119/pdf/WPS7596.pdf.

136 Data sourced from Climate Change Initiative Land Cover, 2019, http://www.esa-landcover-cci.org/?q=node/164.

137 Seidl, R. et al., 2017: Forest disturbances under climate change. *Nature Climate Change*, 7(6): 395–402, https://www.nature.com/articles/nclimate3303.

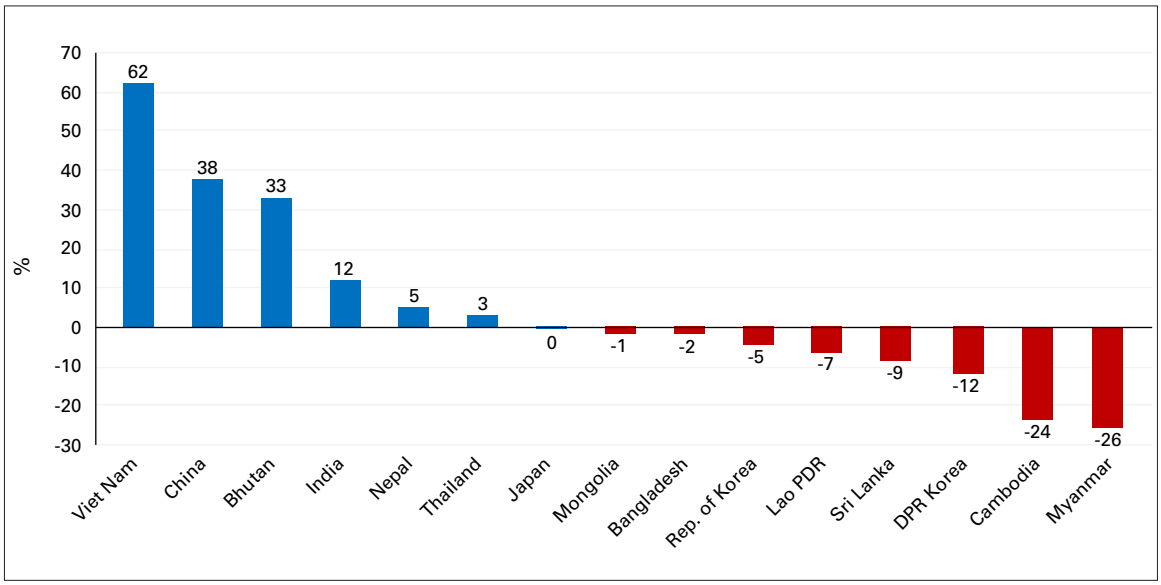

Figure 23. Percentage of change in forest cover 1990–2018. Data sourced from the World Bank and FAO (https://data.worldbank.org/indicator/AG.LND.FRST.ZS).

2018, Viet Nam, China, Bhutan and India, among others, increased their forest cover, whereas decline in forest cover was observed in Myanmar (26%), Cambodia (24%) and the Democratic People's Republic of Korea (12%), among others (Figure 23).

2.2.4 CLIMATE-RELATED HEALTH RISKS

Climate change can adversely affect human health by increasing exposure and vulnerability to extreme weather events and by decreasing the capacity of health systems to adapt to climate conditions.[138] It is reported that temperature increases have been associated with increased incidence of diarrhoeal diseases in East Asia and South Asia, and dengue outbreaks in South and South-East Asia.[139]

In Asia, malaria cases have gradually decreased since 2000. However, dengue cases were widely reported in several countries with an increase in the total number of cases in Asia. In September 2020, a total of 9 108 dengue cases with 14 deaths were reported in Cambodia.[140] Pakistan reported 5 758 confirmed cases of dengue fever with 10 associated deaths. Among those, Sindh province reported the highest number (4 089 cases; 71% of the total), followed by Balochistan province (18%).[141] In Viet Nam, a total of 70 585 dengue cases with seven deaths were reported as 13 September 2020.[142] Yemen also witnessed a rapid increase of dengue cases, from about 24 000 in 2018 (weeks 1–44) to about 60 000 in 2020 (weeks 1–44).[143]

---

138 Cramer, W. et al., 2014: Detection and attribution of observed impacts. In: *Climate Change 2014: Impacts, Adaptation, and Vulnerability. Part A: Global and Sectoral Aspects. Contribution of Working Group II to the Fifth Assessment Report of the Intergovernmental Panel on Climate Change* (C.B. Field et al., eds.). Cambridge, Cambridge University Press, https://www.ipcc.ch/report/ar5/wg2/.

139 Hijioka, Y. et al., 2014: Asia. In: *Climate Change 2014: Impacts, Adaptation, and Vulnerability. Part B: Regional Aspects. Contribution of Working Group II to the Fifth Assessment Report of the Intergovernmental Panel on Climate Change* (V.R. Barros et al., eds.). Cambridge and New York, Cambridge University Press, https://www.ipcc.ch/report/ar5/wg2/.

140 WHO, 2020: Western Pacific Region – Dengue situation update number 606, 22 October, https://reliefweb.int/sites/reliefweb.int/files/resources/Dengue-20201022.pdf.

141 WHO, 2021: Disease outbreaks in the Eastern Mediterranean Region, January to December 2020. *Weekly Epidemiological Monitor*, 14(1), https://reliefweb.int/sites/reliefweb.int/files/resources/2224-4220-2021-1401-eng.pdf.

142 WHO, 2020: Western Pacific Region – Dengue situation update number 606.

143 . Ministry of Public Health and Population, Yemen, 2020: *Weekly Epidemiological Bulletin*, 08(40): 44, https://reliefweb.int/sites/reliefweb.int/files/resources/epidemiological_bulletin_week_44-20204.pdf.

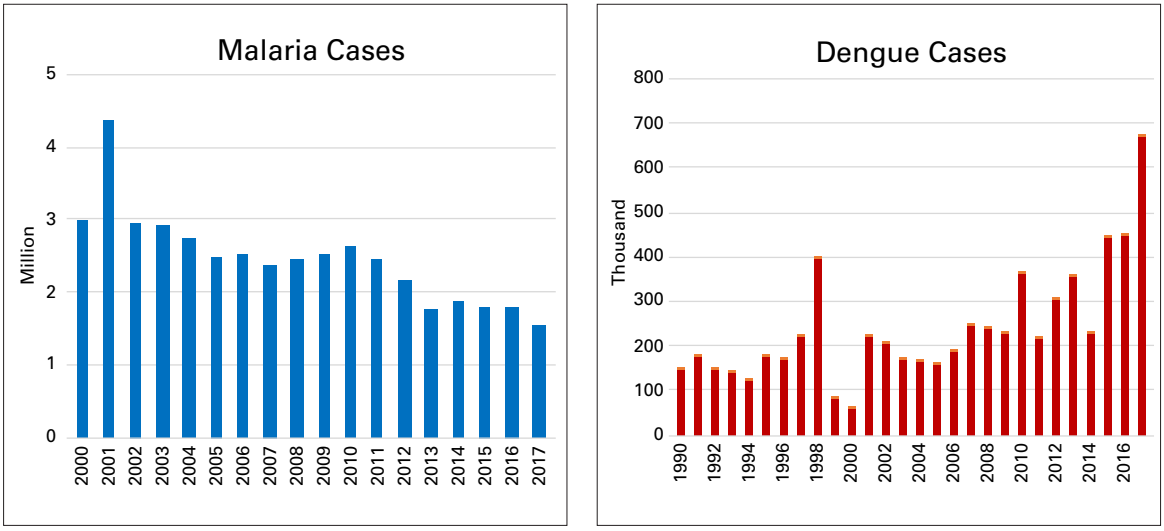

Figure 24. Confirmed malaria and dengue cases in Asia. Data sourced from WHO The Global Health Observatory (https://www.who.int/data/gho/data/themes/topics/topic-details/GHO/cases).

The increase in dengue cases in the region was clearly identified (Figure 24). In particular, from 1990 to 2017, there was a rapid increase of dengue cases in South and South-West Asia, including in Bangladesh, India and Nepal, calling for careful assessment and appropriate measures to address the issue.

2.2.5 BUILD BACK BETTER FOR SUSTAINABLE DEVELOPMENT

Understanding the systemic and cascading risks from extreme climate events

Climate change and the associated increase in natural and biological hazards can exacerbate multidimensional risks for the people and economies of the region. Climate change-driven impacts often act as a threat multiplier to poverty. Moreover, many vulnerable and poor people are dependent on activities, such as agriculture, which can be negatively affected even by small changes in climatic conditions.[144]

The COVID-19 pandemic has highly disrupted socioeconomic development in the region. In South Asia, owing to lockdowns and restrictions on economic activities, it was estimated that up to 132 million people could be pushed into extreme poverty (< US$ 1.90 per day), mostly in India followed by Bangladesh, Pakistan, Nepal and Sri Lanka. Lockdowns have also affected the jobs and livelihoods of millions of internal migrant workers, leading to displacement and a mass exodus to villages.[145]

Asia has regressed on Sustainable Development Goal 13 (Climate Action) in most of its subregions, with varying degrees. It is reported that East and North-East Asia, North and Central Asia, and South-East Asia need to reverse the current trends in order to achieve target 13.1 on climate resilience and adaptive capacity, as well as other resilience targets (target 1.5 and target 11.5).[146] The region is likely to miss the Goals unless efforts are accelerated to build resilience.

It is essential to build resilience to extreme climate events, such as tropical cyclones/typhoons, floods and droughts, especially in high-risk and low-capacity parts of the region, for resilient recovery from the pandemic and for achieving the 2030 Agenda for Sustainable Development. This requires a better understanding of risks, as well as capitalizing on frontier technologies, investing in health and

144 IPCC, 2018: *Global Warming of 1.5°C*

145 ESCAP, 2021: Subregional cooperation to build back better from crises in Asia and the Pacific (ESCAP/77/3), https://www.unescap.org/sites/default/d8files/event-documents/ESCAP_77_3_E.pdf.

146 ESCAP, 2021: *Asia and the Pacific: SDG Progress Report 2021*. Bangkok, United Nations, https://www.unescap.org/sites/default/d8files/knowledge-products/ESCAP_Asia_and_the_Pacific_SDG_Progress_Report_2021.pdf.

social protection and ensuring targeted and forward-looking fiscal spending.[147] Pandemic recovery is also a crucial opportunity for investment in renewable energy.

Understanding and monitoring climate drivers at a regional scale

The July 2020 rainfall event in Japan was triggered by the extreme East Asian summer monsoon rainfall along the Meiyu/Baiu/Changma rain belt during June–July 2020. A tropical Indo-Pacific large-scale thermal condition with a pronounced SST warming in the Indian Ocean basin in a developing La Niña state, compounded by a long-lasting and quasi-stationary Madden-Julian Oscillation activity, created favourable conditions for the extreme rainfall in the region.[148] In the same context, of the East Asian summer monsoon, the chance of occurrence of an event comparable to or exceeding the record-breaking precipitation in the middle and lower reaches of the Yangtze River in China under similar atmospheric circulation conditions is estimated to have increased by five times under the present climate (1985–2019; 6.25%), compared with the past climate (1960–1984; 1.23%). In other words, 80% of the current occurrence probability can be attributed to climate change.[149] Modification of the hydrological cycle is also influenced by human-driven changes or activities, such as land use, land-cover change and modification in river morphology and water table depth.[150]

Adapting to extreme events with early warning systems

Adaptation measures, such as the implementation of early warning systems (EWS) are a key component of reducing Asia's exposure and vulnerability to hydrometeorological hazards. According to the 2020 State of Climate Services report[151], Asia is currently well placed to respond to extreme weather events and is among the regions with the greatest EWS capacity. The report highlights Asia as being particularly advanced in terms of understanding risks, forecasting, and being prepared to respond, with capacities exceeding the global average. Additionally, capacities in preparedness and response are much higher than the global average. Of the countries for which data are available, 35% reported having a multi-hazard early warning system (MHEWS) in place, covering 70 000 in 100 000 on average with early warnings (Figure 25). Monitoring and evaluation of the socio-economic benefits of MHEWS is the area with the lowest percentage of implementation (Figure 26). Systematic documentation of such benefits is essential for attracting investment and ensuring MHEWS sustainability.

It is important to note, however, that data was only obtained from only 56% of the region (19 out of 34 countries), covering about 38% and 50% of Least Developed Countries and Small Island Developing States in the region, respectively. There is thus a substantial need for improved data from all countries in the region to obtain a clearer picture of the gaps and needs moving forward for Asia as a whole.

147 ESCAP, 2021: *Asia-Pacific Disaster Report 2021: Resilience in a Riskier World – Managing Systemic Risks for Biological and Other Natural Hazards* (ESCAP/CDR/2021/1), https://www.unescap.org/knowledge-products-series/asia-pacific-disaster-report.

148 Zhang, W. et al., 2021: Exceptionally persistent Madden-Julian Oscillation activity contributes to the extreme 2020 East Asian summer monsoon rainfall. *Geophysical Research Letters*, 48(5): e2020GL091588, https://doi.org/10.1029/2020GL091588.

149 Ye, Y. and C. Qian, 2021: Conditional attribution of climate change and atmospheric circulation contributing to the record-breaking precipitation and temperature event of summer 2020 in southern China. *Environmental Research Letters*, 16: 044058, https://doi.org/10.1088/1748-9326/abeeaf.

150 IPCC, 2018: *Global Warming of 1.5°C*.

151 https://library.wmo.int/doc_num.php?explnum_id=10385

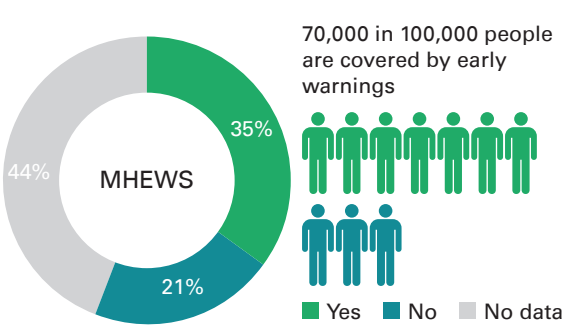

Figure 25. (left) WMO Members that reported having a MHEWS in place, as a percentage of the total number of WMO Members in the region (34). *Source:* WMO, 2020 State of Climate Services (WMO-No. 1252)

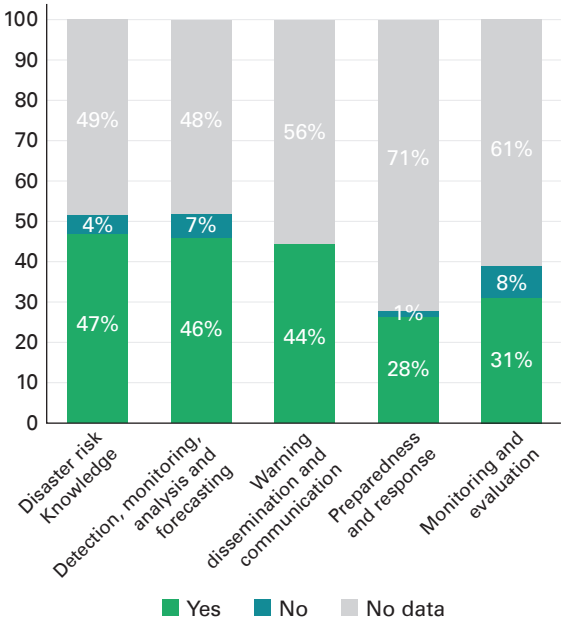

Figure 26. (right) EWS capacities in Asia, by value chain component, calculated as a percentage of functions satisfied in each component area, across 34 WMO Members in the region. *Source:* WMO, 2020 State of Climate Services (WMO-No. 1252)

Climate services for addressing priorities identified in Asian countries' Nationally Determined Contributions to the Paris Agreement

Climate-sensitive sectors such as agriculture, water resources, health and energy, as well as disaster risk reduction are top priorities in the Nationally Determined Contributions (NDCs) submitted by Parties to the United Nations Framework Convention on Climate Change as part of implementation of the Paris Agreement. Decision- and policy-makers concerned with promoting improved climate-related outcomes in these sectors require specialized, sector-specific information.

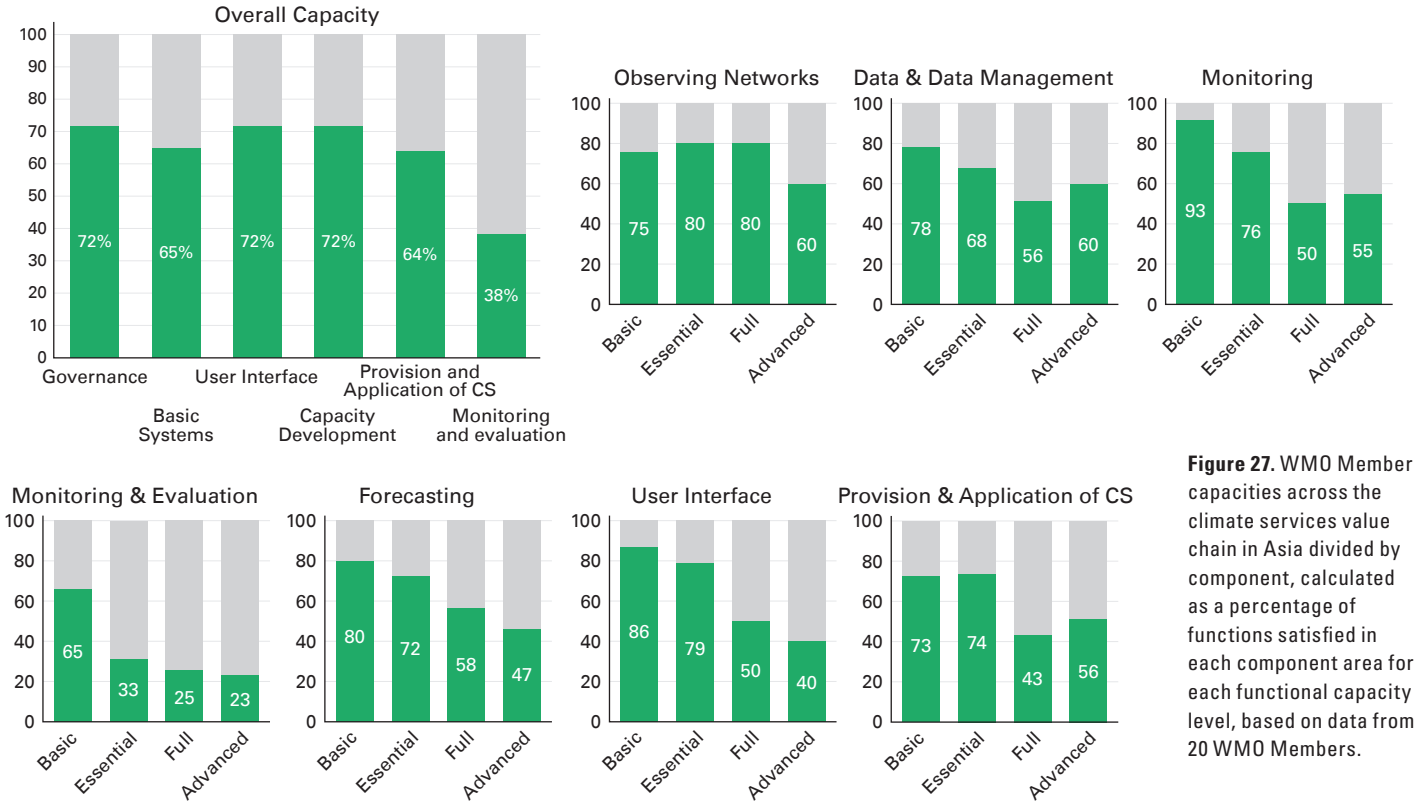

Figure 27. WMO Member capacities across the climate services value chain in Asia divided by component, calculated as a percentage of functions satisfied in each component area for each functional capacity level, based on data from 20 WMO Members.

WMO classifies climate services capacities into four categories: basic, essential, full and advanced. According to the most recent data, 47% of Asian countries are providing services at least at the essential level (Figure 27).

Guidance on implementation of climate services, and specifically for the priority sectors identified in many Asian countries' NDCs is provided by the Global Framework for Climate Services (Priority Areas | GFCS (wmo.int)). Asian country NDCS in particular highlight needs to strengthen data, forecasting and observing networks, and capacity development. These needs are addressed through GFCS guidance on strengthening the constituent components of climate information systems (Components of GFCS | GFCS (wmo.int)) GFCS implementation at national level can be initiated or strengthened through the establishment of National Frameworks for Climate Services (National Frameworks for Climate Services | GFCS (wmo.int)).

Enhancing funding for observational infrastructure

In areas with few observations, weather forecasts and climate monitoring will be of poor and unverifiable quality. There are still major gaps in the availability of climate observations in the region, particularly in South and South-West Asia. WMO's Global Basic Observing Network (GBON) is a network with prescribed capabilities and mandatory international data exchange, established to ensure an adequate supply of surface-based observations needed for numerical weather prediction and climate analysis and reanalysis. Recognizing the need for financial and technical assistance to support the implementation of GBON in the poorest and most poorly observed areas of the globe, WMO and the members of the Alliance for Hydromet Development[152] are establishing the Systematic Observations Financing Facility (SOFF).[153] SOFF will provide long-term support for the collection and sharing of weather and climate observations in compliance with GBON and thereby contribute to improved weather and climate prediction products that underpin 'last mile' adaptation and resilience development projects and programmes.

152 WMO, 2021: Alliance for Hydromet Development, https://public.wmo.int/en/our-mandate/how-we-do-it/partnerships/wmo-office-of-development-partnerships.

153 WMO, 2021: Systematic Observations Financing Facility, https://public.wmo.int/en/our-mandate/how-we-do-it/development-partnerships/Innovating-finance.

LIST OF CONTRIBUTORS

CONTRIBUTING EXPERTS:

PART I:

Atsushi Goto (Japan, lead of Part I), Peiqun Zhang (China, lead of Part I), Yasushi Takatsuki (Japan, Chairperson of RA II Working Group on Climate Services), Bo LU, Pengling Wang, Lijuan MA (China, RCC Beijing), Valentina Khan (Russian Federation, RCC Moscow), D.S. Pai, O.P. Sreejith (India, RCC Pune), Koichiro Kakihara, Shunya Wakamatsu (Japan, RCC Tokyo), Yeonhee Kim, Jinwon Kim, Seontae Kim (Republic of Korea), Ahad Vazifeh, Sadegh Zeyaeyan (Iran, Islamic Republic of), Phuc Lam Hoang (Viet Nam), Noura al Hameli (United Arab Emirates), Abdulkarem Almashi, Shekha Alseari (Saudi Arabia), John Kennedy (MetOffice, United Kingdom of Great Britain and Northern Ireland), Markus Ziese (GPCC, Germany), Anny Cazenave (Legos, France), Karina Von Shuckmann (Mercator-Ocean, France), Juerg Lutherbacher, José Álvaro Silva (WMO)

PART II:

Sanjay Srivastava (Lead of Part II), SungEun Kim (Lead of Part II), Sapna Dubey, Maria Dewi, Jaehee Hwang, Ranhee Kim, Seungwon Hyun (The Economic and Social Commission for Asia and the Pacific (ESCAP)), Hideki Kanamaru, Hang Thi Thanh Pham, Beau Damen, Catherine Jones, Kaustubh Devale, Kara Jenkinson, Thai Anh Nguyen (The Food and Agriculture Organization (FAO)), Jothiganesh Shanmugasundaram, Almudena Serrano (The World Food Programme (WFP)), Florence Geoffroy, Katja Susanna Rytkoenen (The Office of the United Nations High Commissioner for Refugees (UNHCR)), Maria Angenieta Veger, Chandan Nayak, Anny Yip-Ching Yu, Nizamudin Haidari (included by FAO) (International Organization for Migration (IOM)), Maxx Diley, Omar Baddour, Filipe Lucio, Veronica Grasso, Nakiete Msemo, Claire Ramson (WMO)

EXPERT TEAM ON CLIMATE MONITORING AND ASSESSMENT (REVIEWERS):

John Kennedy (Lead, United Kingdom of Great Britain and Northern Ireland), Jessica Blunden (Co-lead, United States of America), Awatif Ebrahim Mostafa (Egypt), Ardhasena Sopaheluwakan (Indonesia), Ladislaus Benedict Chang'a, (United Republic of Tanzania), Freja Vamborg (ECMWF), Randall S. Cerveny (United States of America), Serhat Sensoy (Turkey), Zhiwei Zhu (China), Blair Trewin (Australia), Jose Luis Stella (Argentina), Liudmila Kolomeets (Russian Federation), Renata Libonati (Brazil)

CONTRIBUTING NATIONAL METEOROLOGICAL, HYDROMETEOROLOGICAL AND HYDROLOGICAL SERVICES:

Bahrain Meteorological Service (Bahrain), China Meteorological Administration (China), Hong Kong Observatory (Hong-Kong, China), India Meteorological Department (India), Islamic Republic Of Iran Meteorological Organization (Iran, Islamic Republic of), Japan Meteorological Agency (Japan), Republican State Organization 'Kazhydromet' (Kazakhstan), Department of Meteorology and Hydrology (Myanmar), Pakistan Meteorological Department (Pakistan), Korea Meteorological Administration (Republic of Korea), Russian Federal Service For Hydrometeorology and Environmental Monitoring (ROSHYDROMET) (Russian Federation), Presidency of Meteorology & Environment (PME) (Saudi Arabia), The National Center of Meteorology and Seismology (United Arab Emirates), The Centre of Hydrometeorological Service at Cabinet of Minister's of Republic of Uzbekistan (UZHYDROMET) (Uzbekistan), Hydro-Meteorological Service of Vietnam (Viet Nam)

DATASET DETAILS

TEMPERATURE DATA

Regional mean temperature is reported as the mean of the six data sets listed below. Regional mean temperature anomalies are expressed relative to the 1981–2010 average.

The averages for the NOAAGlobalTemp and GISTEMP data sets are set equal to that of HadCRUT4 over the period 1880–1900 and the averages for the two reanalyses are set to equal that of HadCRUT4 over the period 1981–2010. HadCRUT4 is used as a basis for aligning other data sets for consistency with the global reports.

HADCRUT.5.0.1.0

Morice, C.P. et al., 2021. An updated assessment of near-surface temperature change from 1850: The HadCRUT5 data set. *Journal of Geophysical Research: Atmospheres*, 126(3): e2019JD032361, https://doi.org/10.1029/2019JD032361. HadCRUT.5.0.1.0 data were obtained from http://www.metoffice.gov.uk/hadobs/hadcrut5 on 14 February 2021 and are © British Crown Copyright, Met Office 2021, provided under an Open Government Licence, http://www.nationalarchives.gov.uk/doc/open-government-licence/version/3/.

NOAAGLOBALTEMP V5

Zhang, H.-M. et al., 2019: *NOAA Global Surface Temperature Dataset (NOAAGlobalTemp), version 5.0*. NOAA National Centers for Environmental Information. DOI:10.7289/V5FN144H, https://www.ncei.noaa.gov/access/metadata/landing-page/bin/iso?id=gov.noaa.ncdc:C00934.

Huang, B. et al., 2020: Uncertainty estimates for sea surface temperature and land surface air temperature in NOAAGlobalTemp version 5. *Journal of Climate*, 33(4): 1351–1379, https://journals.ametsoc.org/view/journals/clim/33/4/jcli-d-19-0395.1.xml.

GISTEMP V4

GISTEMP Team, 2019: *GISS Surface Temperature Analysis (GISTEMP), version 4*. National Aeronautics and Space Administration (NASA) Goddard Institute for Space Studies, https://data.giss.nasa.gov/gistemp/.

Lenssen, N.J.L. et al., 2019: Improvements in the GISTEMP uncertainty model. *Journal of Geophysical Research: Atmospheres*, 124(12): 6307–6326, https://doi.org/10.1029/2018JD029522.

BERKELEY EARTH

Rohde, R.A. and Z. Hausfather, 2020: The Berkeley Earth land/ocean temperature record. *Earth System Science Data*, 12: 3469–3479, https://doi.org/10.5194/essd-12-3469-2020.

ERA5

Hersbach, H. et al., 2020: The ERA5 global reanalysis. *Quarterly Journal of the Royal Meteorological Society*, 146(730): 1999–2049, https://doi.org/10.1002/qj.3803.

JRA-55

Kobayashi, S. et al., 2015: The JRA-55 reanalysis: general specifications and basic characteristics. *Journal of the Meteorological Society of Japan*, 93(1): 5–48, https://www.jstage.jst.go.jp/article/jmsj/93/1/93_2015-001/_article.

PRECIPITATION DATA

Regional time series analyses of the area-mean annual precipitation totals are from the Global Precipitation Climatology Centre (GPCC). Regional precipitation anomalies are expressed relative to the 1981–2010 average.

Schneider, U. et al., 2020: *GPCC Monitoring Product: Near Real-Time Monthly Land-Surface Precipitation from Rain-Gauges Based on SYNOP and CLIMAT Data*. DOI: 10.5676/DWD_GPCC/MP_M_V2020_100, https://opendata.dwd.de/climate_environment/GPCC/html/gpcc_monitoring_v2020_doi_download.html.

SEA-ICE DATA

In this report, the estimation of sea-ice extent is based on an analysis of blended Arctic ice charts from the Arctic and Antarctic Research Institute (Russian Federation), the Canadian Ice Service (Canada) and the National Ice Center (United States of America) using passive microwave estimates (SMMR, SSM/I and SSMIS) from the National Snow and Ice Data Center.


For more information, please contact:

World Meteorological Organization

7 bis, avenue de la Paix – P.O. Box 2300 – CH 1211 Geneva 2 – Switzerland

Strategic Communications Office

Tel.: +41 (0) 22 730 83 14 – Fax: +41 (0) 22 730 80 27

Email: communications@wmo.int

public.wmo.int

JN 211126